Experience of MRCAT in Radiotherapy for Prostate Cancer

Sang Hoon Jung, Ph.D,

Clinical Assistant Professor / Medical Physicist
Department of Radiation Oncology, Samsung Medical Center

Location of SMC (Dept. Radiation Oncology)

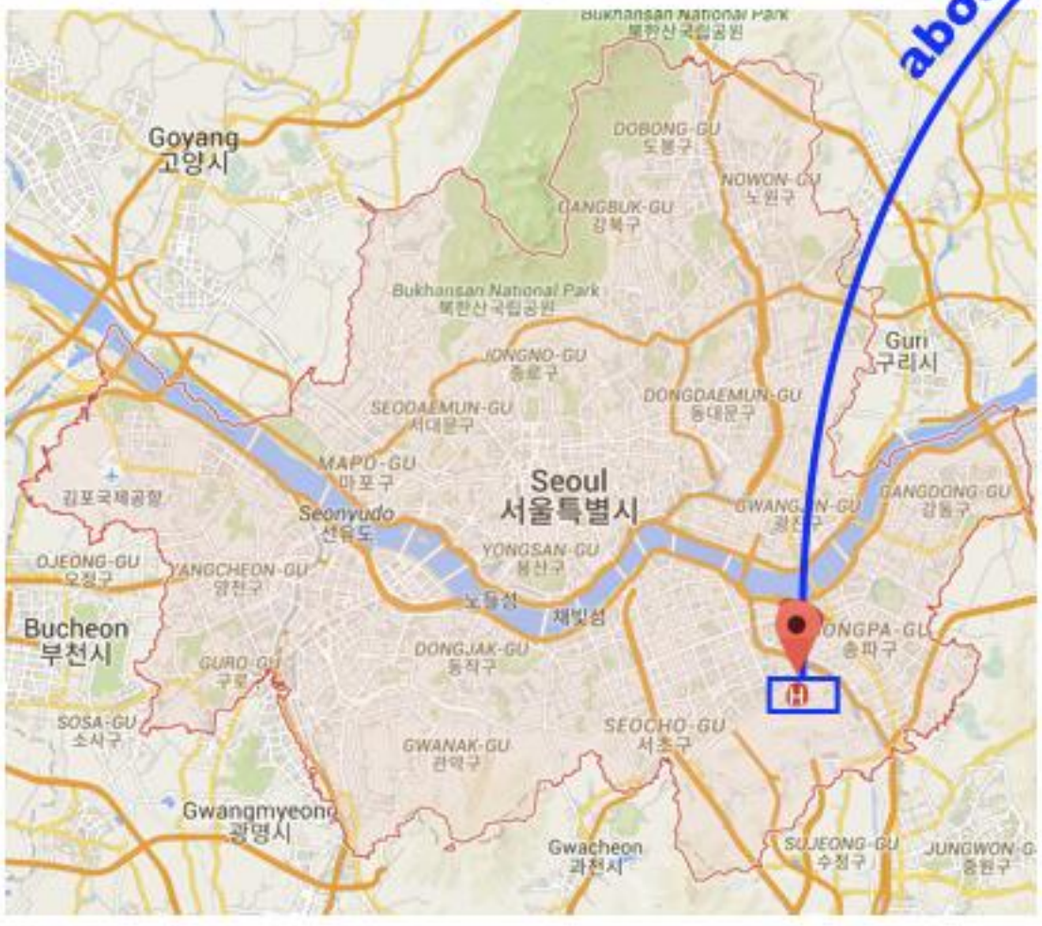

Comprehensive Cancer Center
B1

Proton Center
B1 ~ B3

SAMSUNG MEDICAL CENTER

Resources in SMC




1994	2002	2008	2016
2 Faculty (MD)	4 Faculty (MD)	6 Faculty (MD)	11 Faculty (MD)
1 Physicist Faculty	1 Physicist Faculty	1 Physicist Faculty	4+5 Physicist Faculty (+2/+7)
			1 Biologist Faculty
	4 Trainee	10 Trainee	8 Trainee (Resid. & fellow)
9 RTT	18 RTT	35 RTT	56 RTT
19	37	68	121

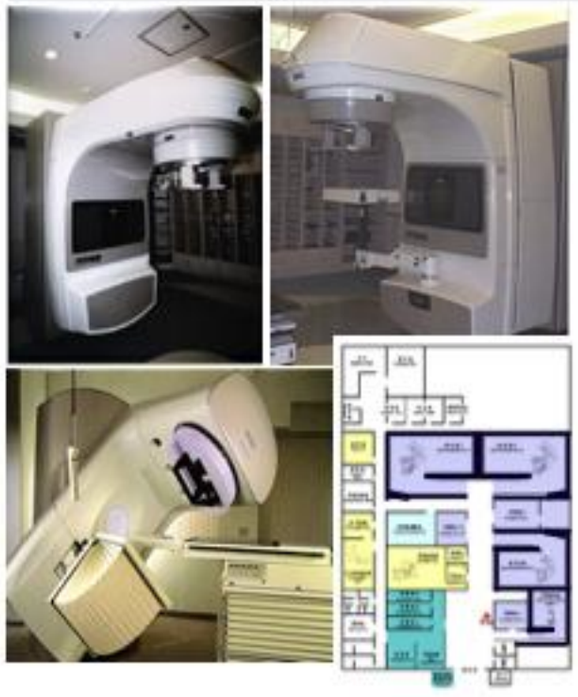


Resources in SMC

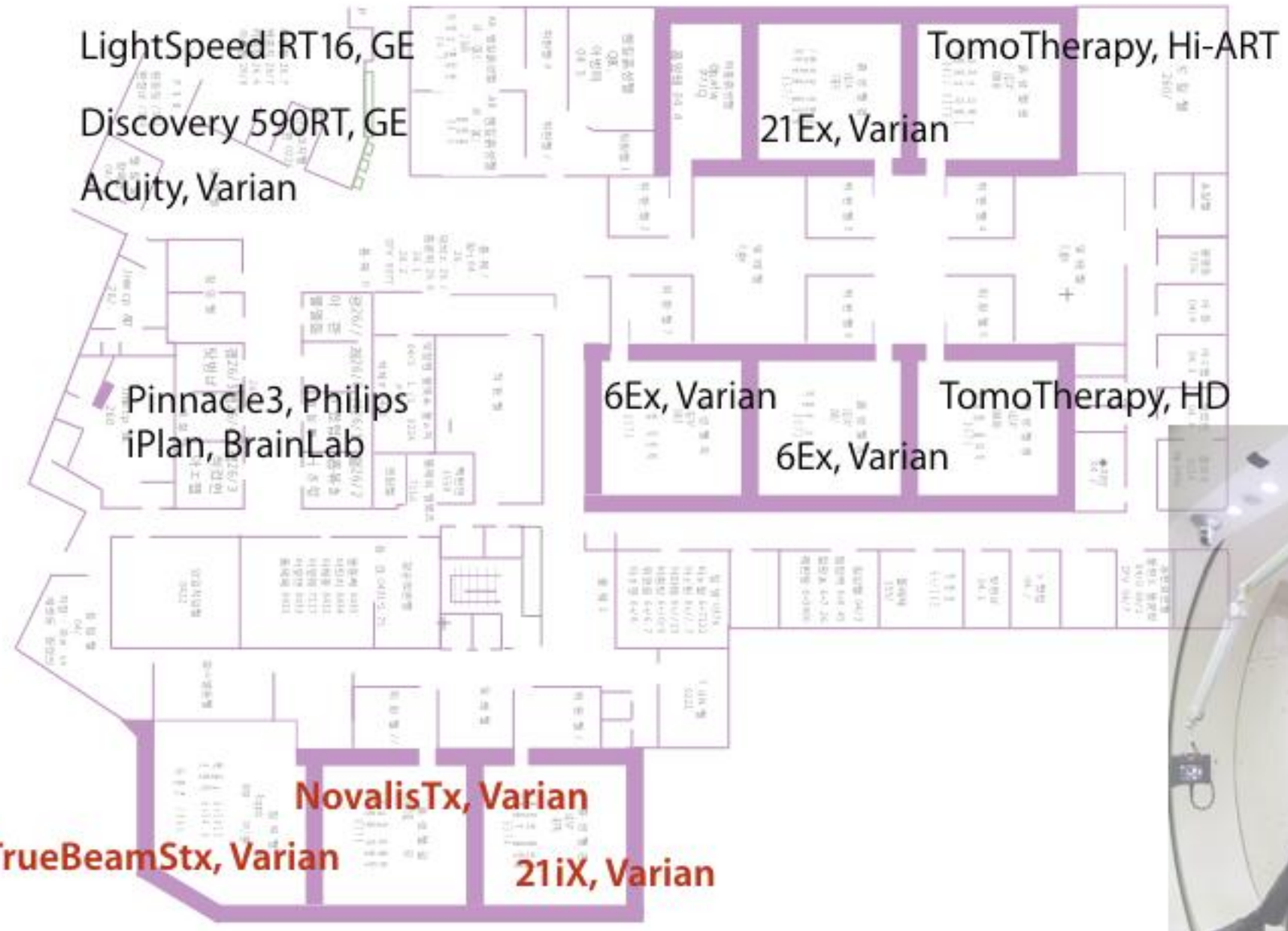

Conventional Simulator: 1
CT simulators: 3
MR-RT simulator: 1
Linacs: 6
TomoTherapies: 2
Gantries with CBCT: 2

Achieva 3.0T MR-RT, Philips

RayStation, RaySearch

Two Gantries with CBCT

Clinical Use of MRI in SMC

- MR-RT simulator, Ingenia 3.0T MR-RT Simulator
- Planning MR
  - The same Set-up of CT simulation
  - Interval Time btw. CT simulation and MR simulation < 1 hr
- Limited use:
  - Delineation of Target and Organs-At-Risk with Rigid Registration

	Use of MRI	Planning MRI
Liver	O	O
Brain	O	
Head & Neck	O	O
Prostate	O	O
Spine	O	O
etc.	O	O

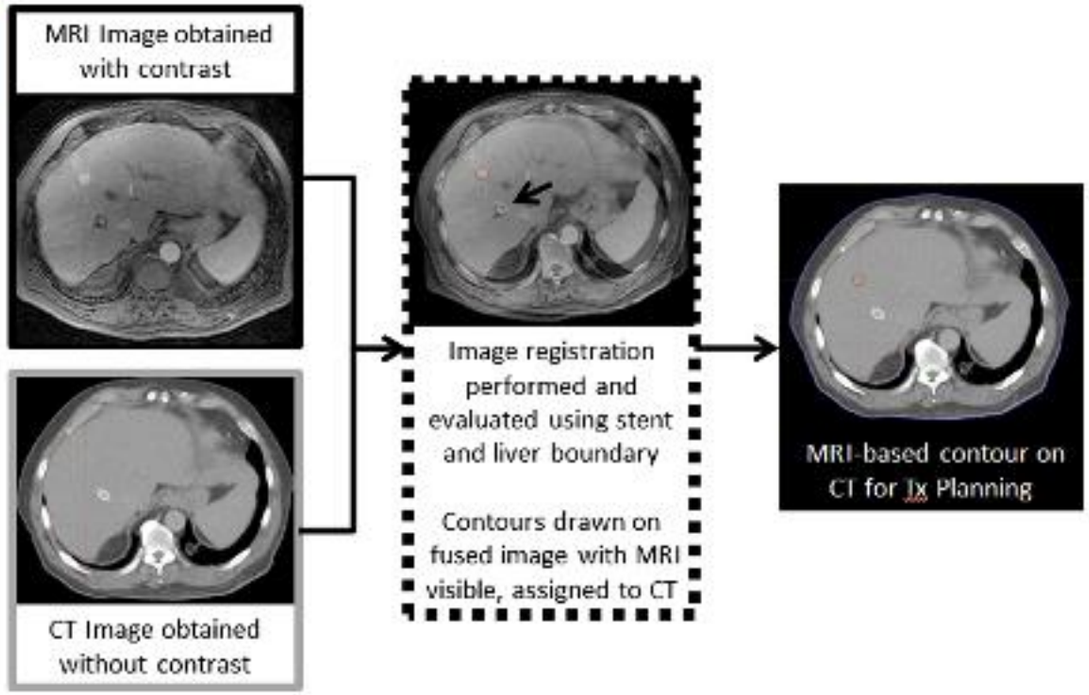

K. K. Brock and L. A. Dawson, Seminars in Radiation Oncology **24**, 169-174 (2014).

Ingenia 3.0T MR-RT Simulator

- **Philips Health Care**
- **Installed at 2015. Apr**
- **MR-RT CouchTop**
- **External Laser Positioning System**
- **MRCAT and 4DMR**
- Anterior Coil Support
- Indexing bars (S) and (L)
- Headrest fixation
- dStream Interface Support
- Wall Mount for storing all the MR-RT components

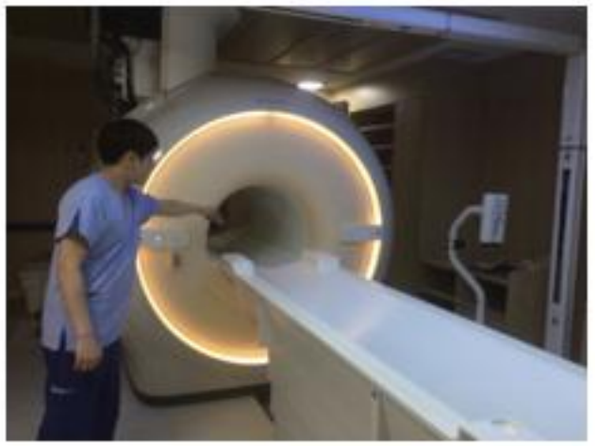

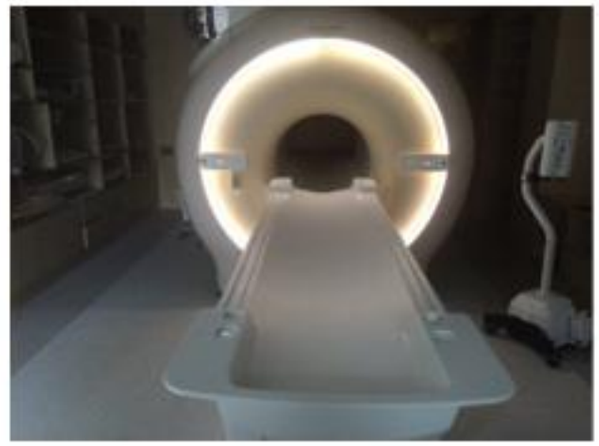

Multi-modal images in radiotherapy

- **Computed Tomography**
  - **Attenuation coefficient**
  - **Energy, imaging protocol, contrast agent**

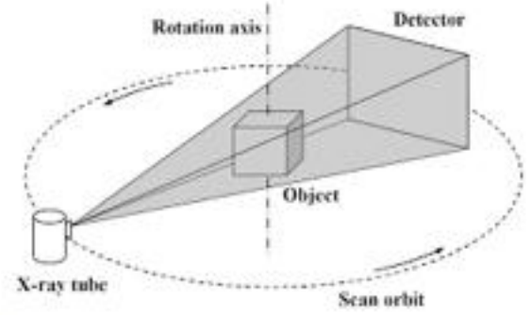

- Postiron Emission Tomography
  - Positron-emitting radionuclide
  - Agent, FDG, MISO, and so on

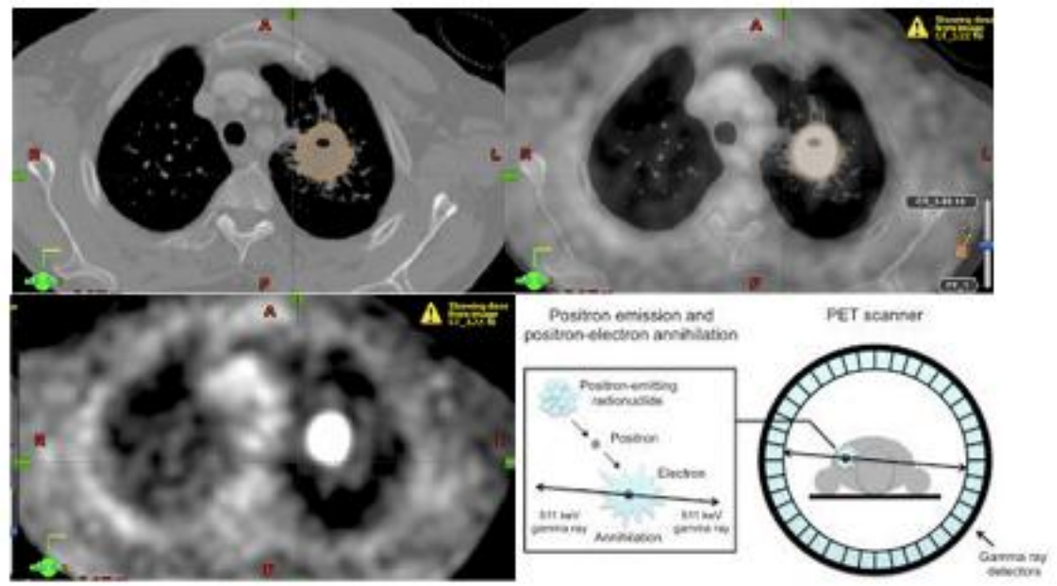

Figure 4 PET/CT fusion role in delineation of tumor. Left: CT image showing gross tumor. Right: PET image showing disease uptake. Middle: PET/CT fusion correlating gross tumor with uptake in PET.

- Magnetic Resonance Imaging
  - Resonance pulse, Relaxation time, and so on
  - Contrast agent, imaging protocols, and so or
- Ultrasound, etc.

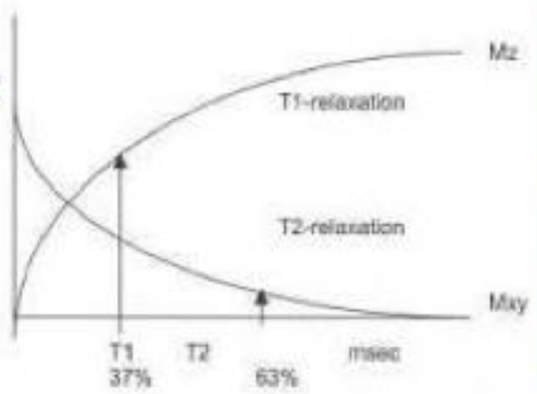

Tissue	T1 (msec)	T2 (msec)
Water/CSF	4000	2000
Gray matter	900	90
Muscle	900	50
Liver	500	40
Fat	250	70
Tendon	400	5
Proteins	250	0.1- 1.0
Ice	5000	0.001

Preliminary image in radiotherapy

- Computed tomography
  - **Electron density converted to attenuation coefficient for radiotherapy**
  - Geometrical accuracy of anatomy
  - **Lack of contrast resolution for differentiation between normal soft tissue structures and tutor extent**
- Advantages of MRI in radiotherapy
  - Superior contrast resolution and better soft tissue differentiation
  - No need - radiation exposure, iodinated contrast agent
  - Functional imaging sequences

	CT	PET	MRI
Signal intensity	Electron density	Uptake	Material composition and uptake
Resolution	Fine	Coarse	Fine
3D imaing	OK	OK	OK
Radiation	Exposure	Exposure	Non-ionizing
Acquisition time	less than 1 min	mins	a few seconds ~ mins (Imaging protocol)
Anatomy	OK	N/A	OK

Image Values of MR to Density (HU)

- Manual Bulk Density Assignment
  - Brain (R. Prabhakar, 2007) and Prostate (J. Lambert, 2011)
  - Mean dose discrepancy less than 3%
- Different Bulky Density
  - Brain: Point Dose < 1% (K. Eilertsen, 2008)
  - Prosate: < 2% (K. Eilertsen, 2008)
- Atlas based synthetic CT (or pseudo CT)
  - Prostate: < 2% (J. A. Dowling, 2012)
- Voxelwise conversion, sCT
  - Brain and Prostate: < 0.5% (J. H. Jonsson, 2013)

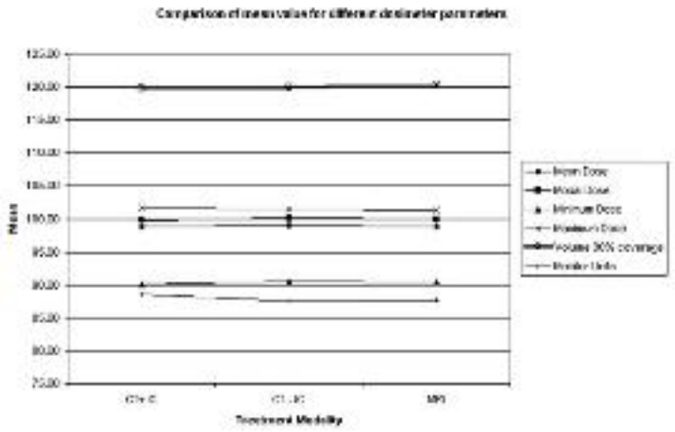

Figure 4. Comparison of mean value for different dosimetric parameters.

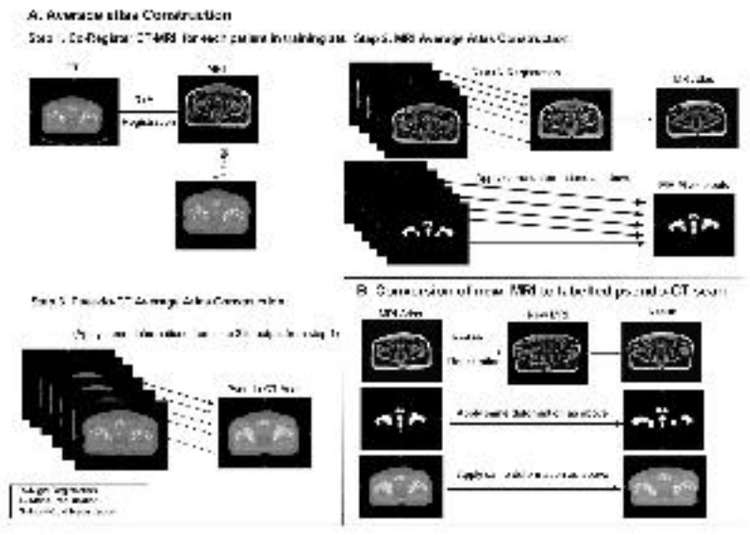

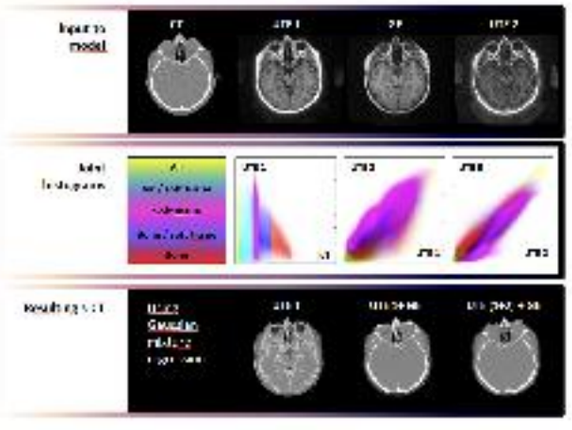

MRCAT: Magnetic Resonance for Calculating ATtenuation

- Dedicated mDIXON FFE
- CT-like density maps are automatically generated with MRCAT post processing algorithm.

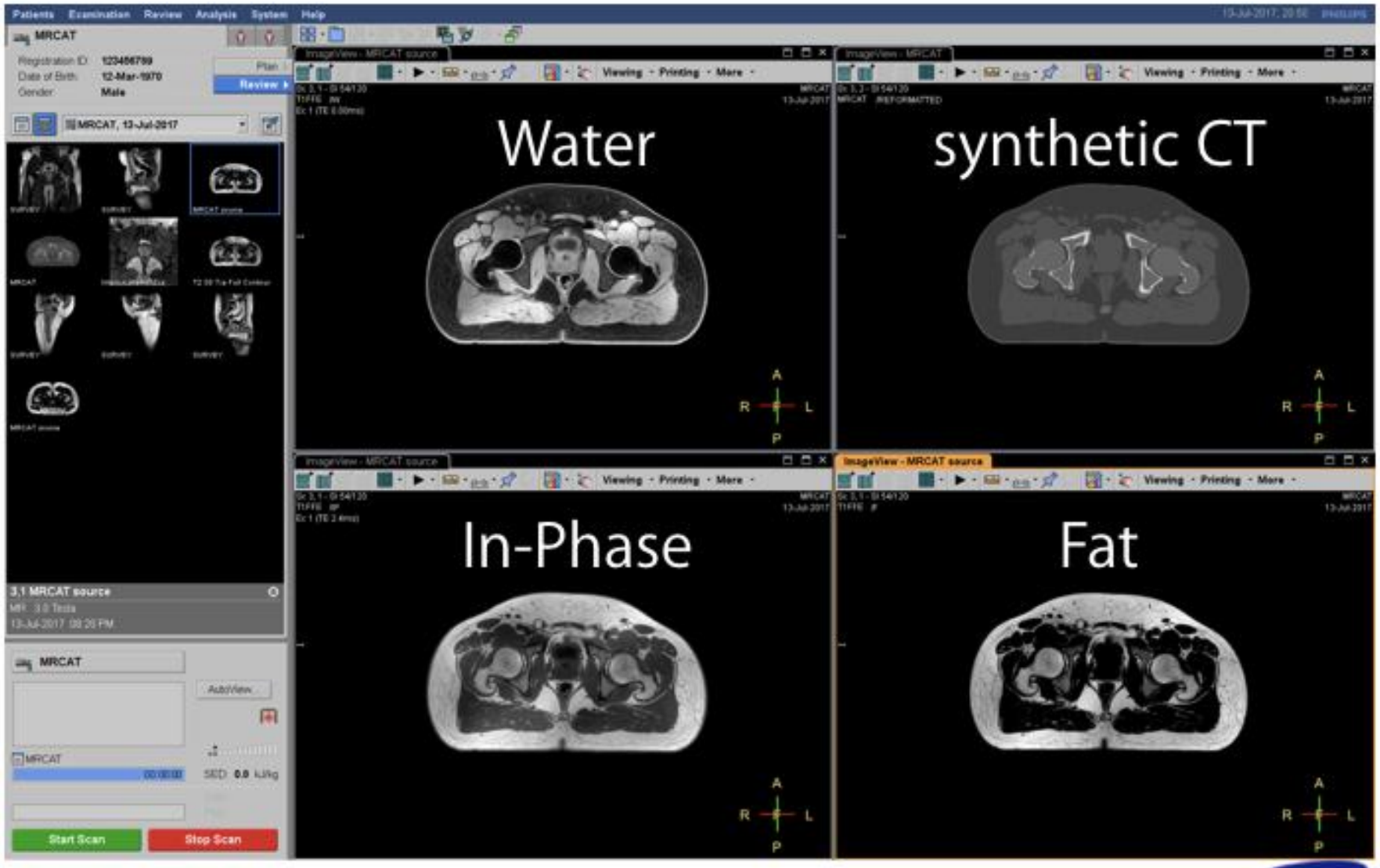

SAMSUNG MEDICAL CENTER

MRCAT Source Image Acquisition

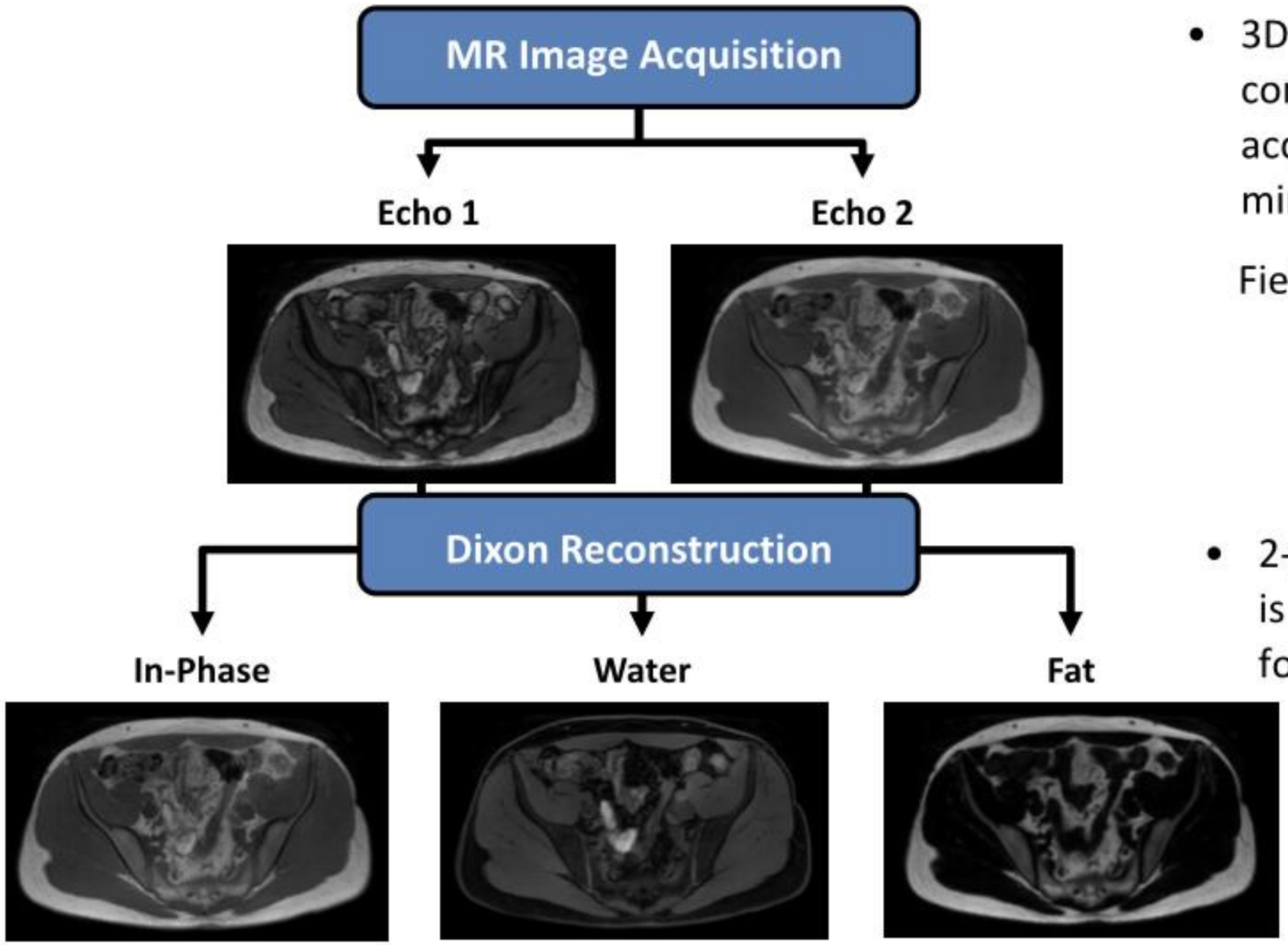

- 3D FFE 2-echo, full body contour large volume scan is acquired in less than three minutes.

  Field-of-View (AP-LR-HF):

  M: 350 x 451 x 300 mm^3

  L: 368 x 552 x 300 mm^3

- 2-point Dixon reconstruction is used to generate the following 3D image sets:

  1. In-phase
  2. Water-only
  3. Fat-only

MRCAT Algorithm Overview

MRCAT source water image

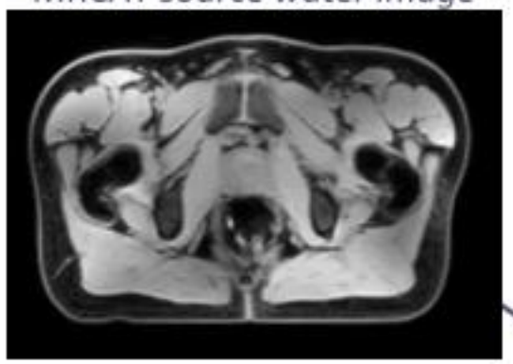

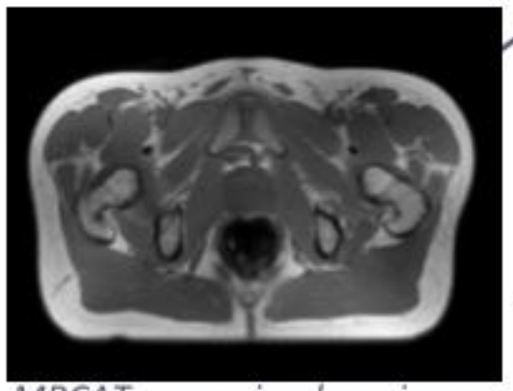

MRCAT source in-phase image

Calculate body mask

Soft tissue classification

Segment bone mask

Classify compact and spongy bone

Assign HU values

MRCAT image

Mask Calculation

mDixon water and in-phase images are used as input for body mask calculation. This segmentation is model based.

Calculate body mask

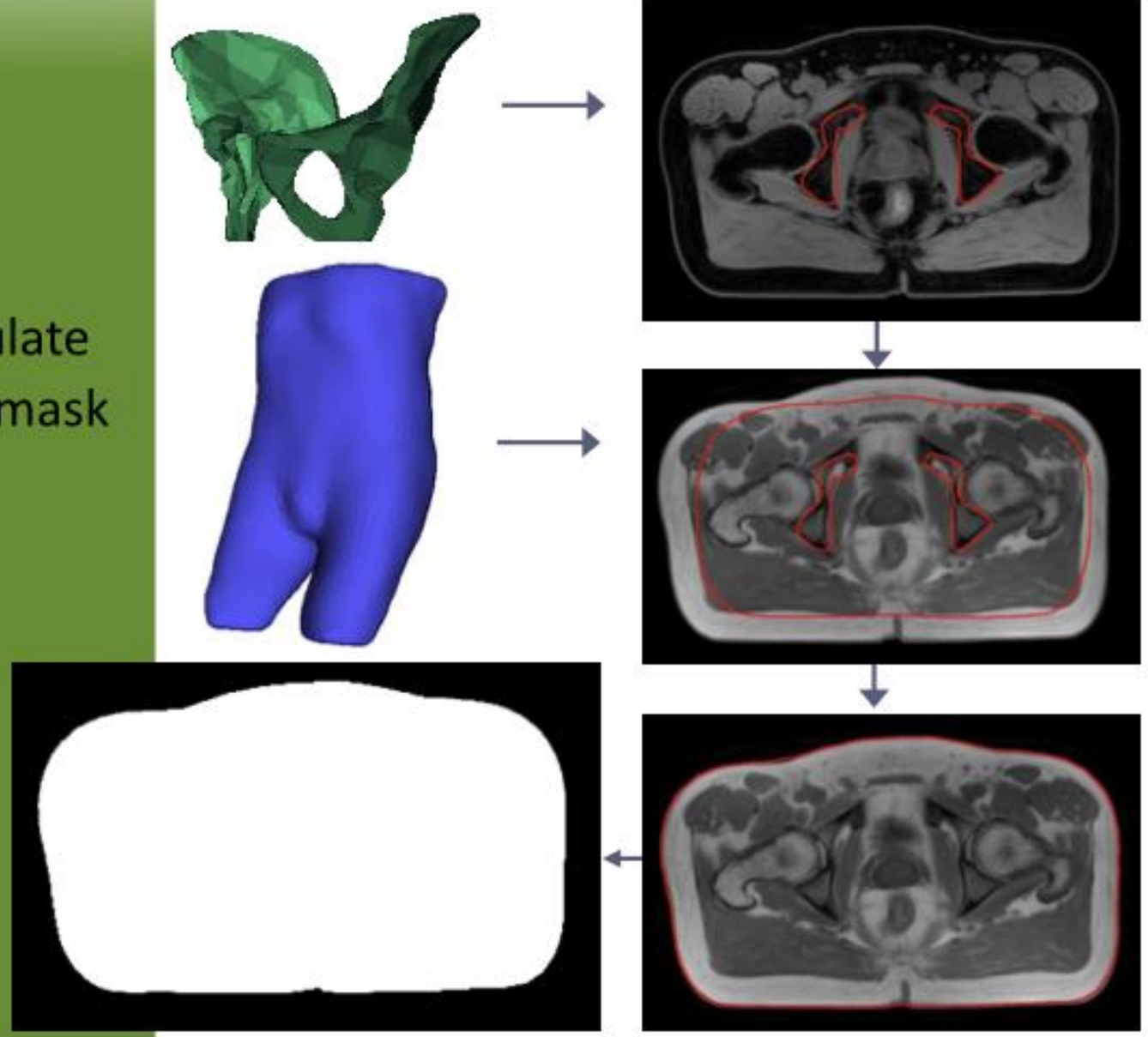

- Pelvic bone model is used to determine the initial position using the water image.
- Result is moved to in-phase image and body outline model is added.
- Adaptation for final body outline is done.
- Body mask from outline is generated.

PHILIPS

4598 009 37281

SAMSUNG MEDICAL CENTER

Soft Tissue Classification

mDixon water and fat images are used as input for soft tissue classification.

Classify soft tissue

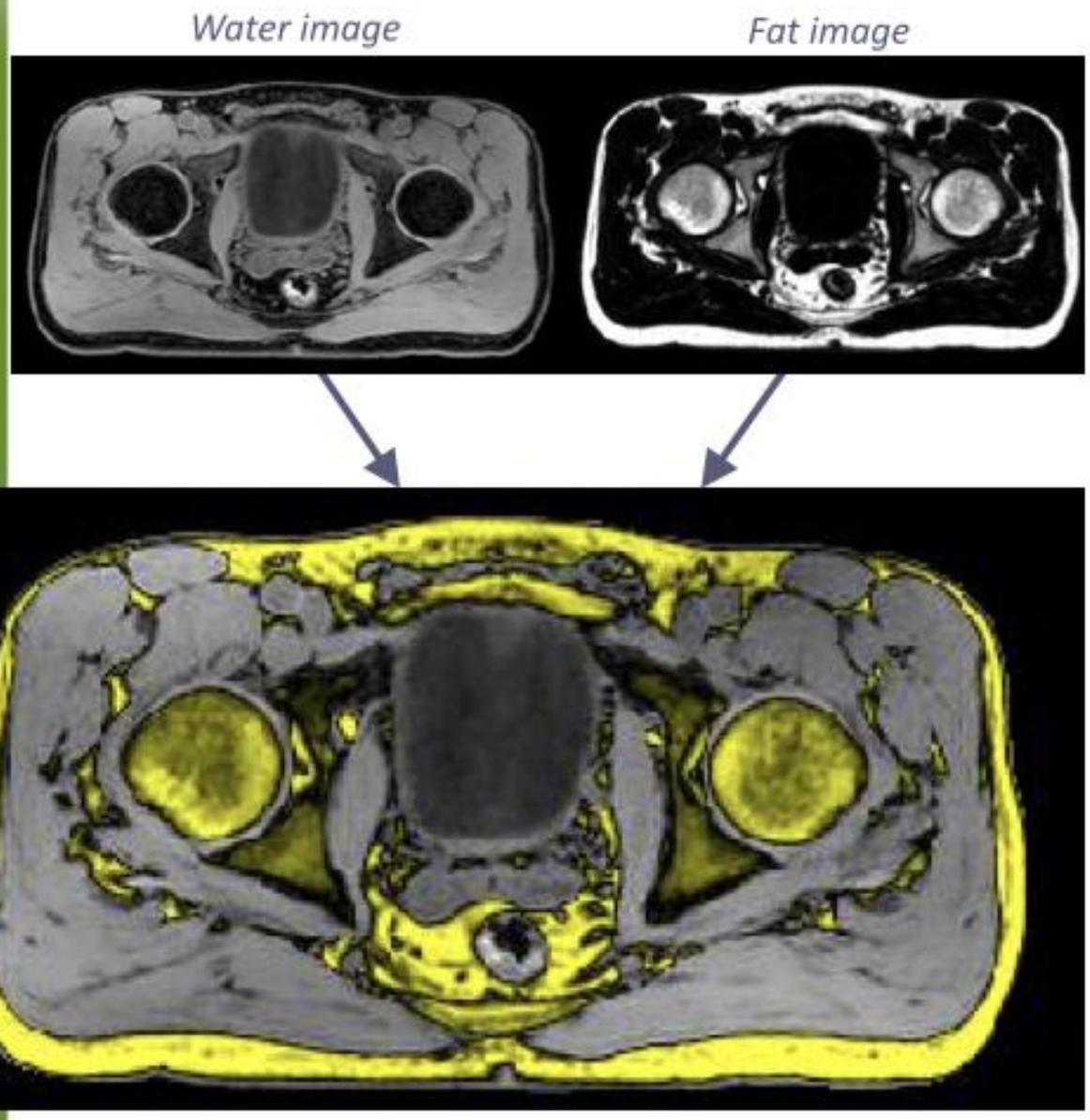

- MRCAT images discern water (muscle) and fatty tissues.

Each voxel inside the body mask is evaluated.

Voxel where
water signal is larger → water
fat signal is larger → fat

Grey → muscle/water
Yellow → fat

PHILIPS
4598 009 37281

SAMSUNG MEDICAL CENTER

Bone Segmentation

Initialization of bone segmentation is similar to body outline adaptation.

Segment bone mask

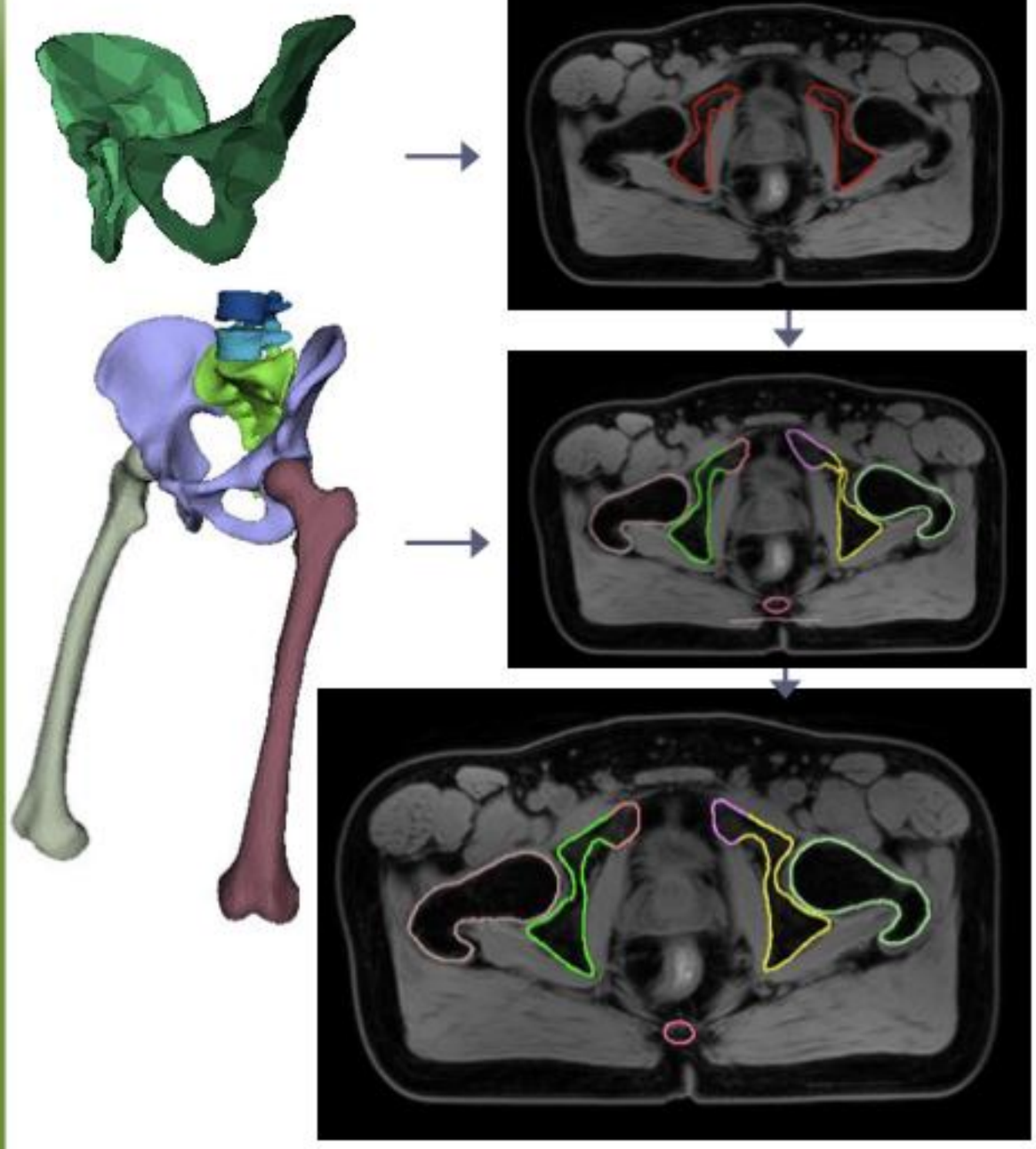

- Initial position of model determined, based on pelvic bone model.
- Remaining bones are added.
- Model based adaptation for water image.

PHILIPS

4598 009 37281

SAMSUNG MEDICAL CENTER

Bone Segmentation

Fine tuning of the bone model with in-phase image.

Segment bone mask

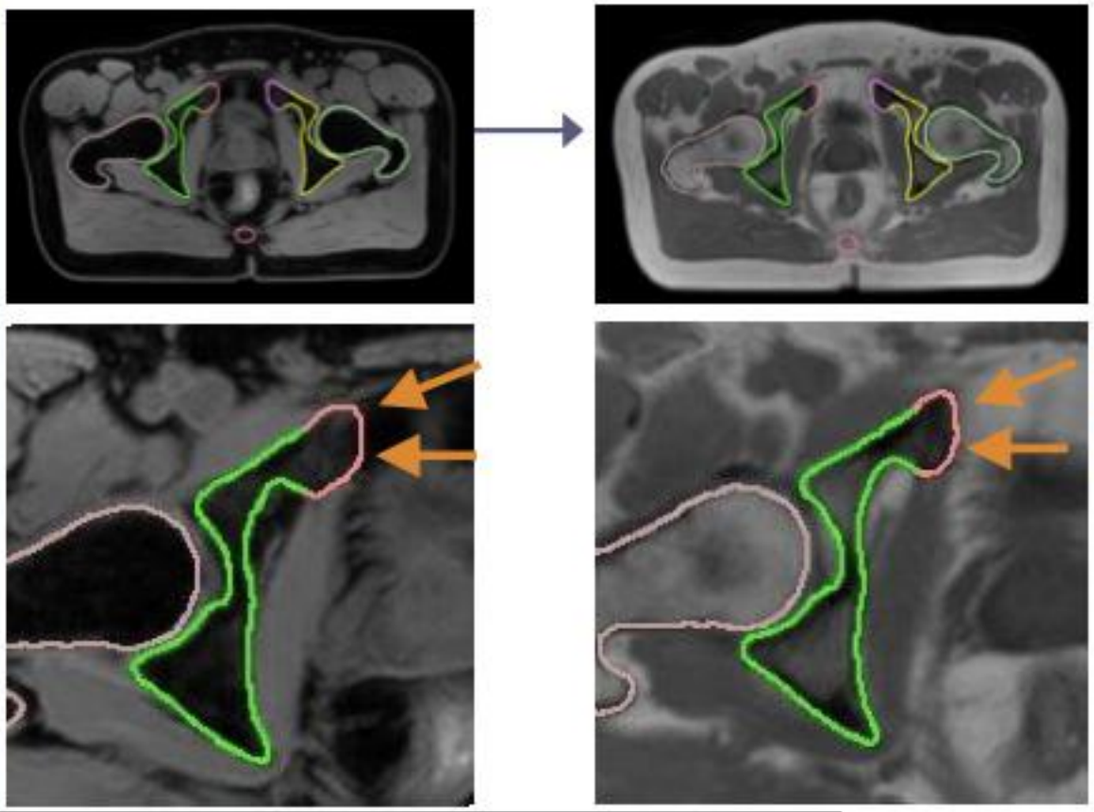

Segmentation result is moved to in-phase image.

- Bone and fat appear similar in water images (dark/black), but are clearly distinguishable in the in-phase image.

➢ Areas where bone is adjacent to fat pockets are often incorrect after water image adaption.

- In-phase image is used to polish.

Bone mask from bone segmentation is generated.

PHILIPS

4598 009 37281

SAMSUNG MEDICAL CENTER

Compact Bone Determination

Classify compact bone

Within the bone mask, voxels with in-phase signal intensity below threshold are classified as compact bone.

In-phase signal intensity above threshold is classified as compact bone.
Areas not classified as compact bone, are classified as spongy bone.

In-phase image

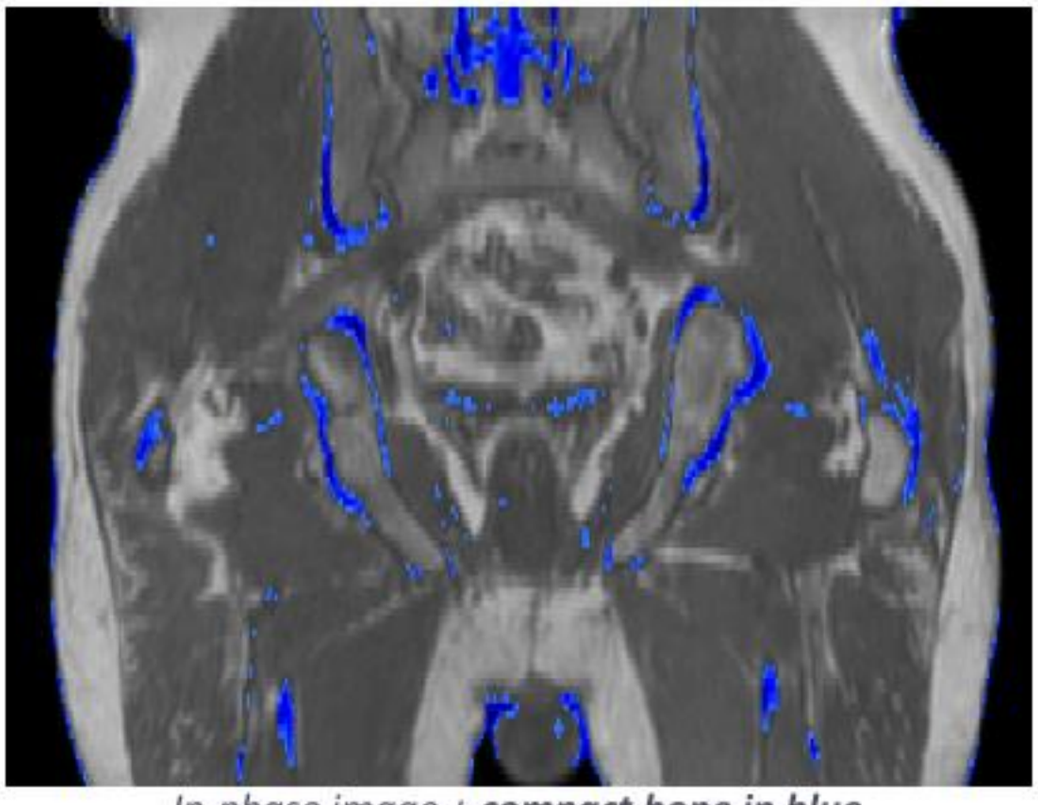

*In-phase image + **compact bone in blue***

PHILIPS

4598 009 37281

SAMSUNG MEDICAL CENTER

HU Value Assignment

Assign class HU values

HU values for each class are assigned.

- Values based on calibration of MRCAT images against true CT images for a cohort of patients.

Tissue	Hounsfield unit
Air/ background	-968
Fat tissue	-86
Other soft tissue	42
Spongy bone	198
Compact bone	949

PHILIPS

4598 009 37281

SAMSUNG MEDICAL CENTER

MRCAT in RT for Prostate Cancer

- To introduce a technique for generating synthetic CT using MRCAT in conventional MR simulator
- 16 patients treated using **TomoTherapy**
  - 16 sets of synCT using MRCAT
  - Comparison of planCT and synCT: parameters in image
    - Image Value
    - Dosimetric Comparison of DVH parameters (Max, Mean, Min), 3D Gamma etc.

Source Images of MRCAT, synCT and planCT

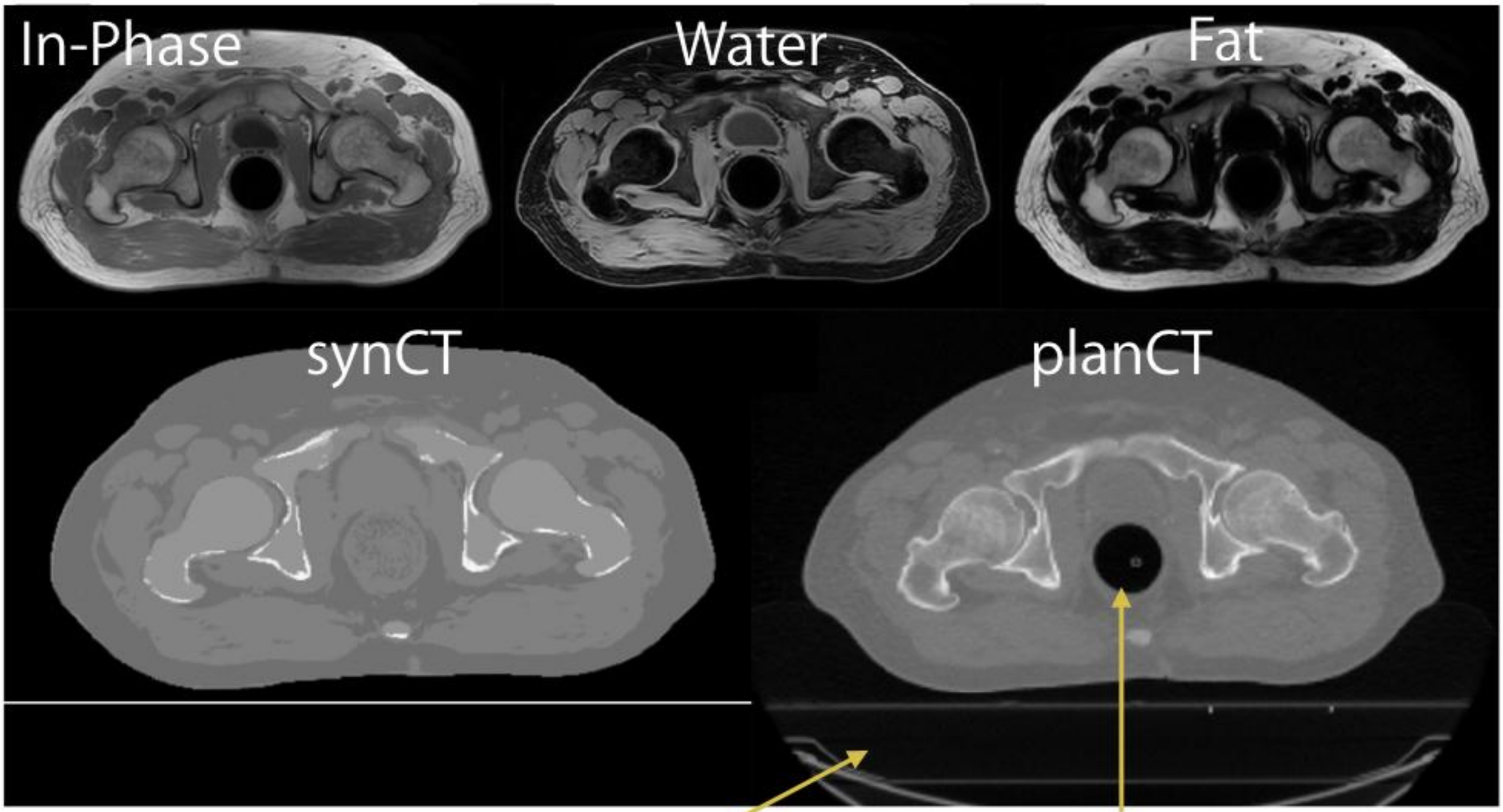

SAMSUNG MEDICAL CENTER

Dose Calculation on synCT in TomoTherapy

- Preprocessing of synCT from MRCAT
  - MIM maestro, ver. 6.4.9 (MIM Software, Cleveland, OH, USA)
  - Rigid Registration of synCT to planCT
  - Dimensions of the synCT image was matched to those of the planCT images
- Dose Calculation using DQA workstation (Accuray Inc., Sunnyvale, CA, USA)
  - Hi-Art® ver. 4.2.3 or TomoHD™ ver. 1.2.3
  - Treatment Plan Optimized using planCT

Examples of synCT and planCT

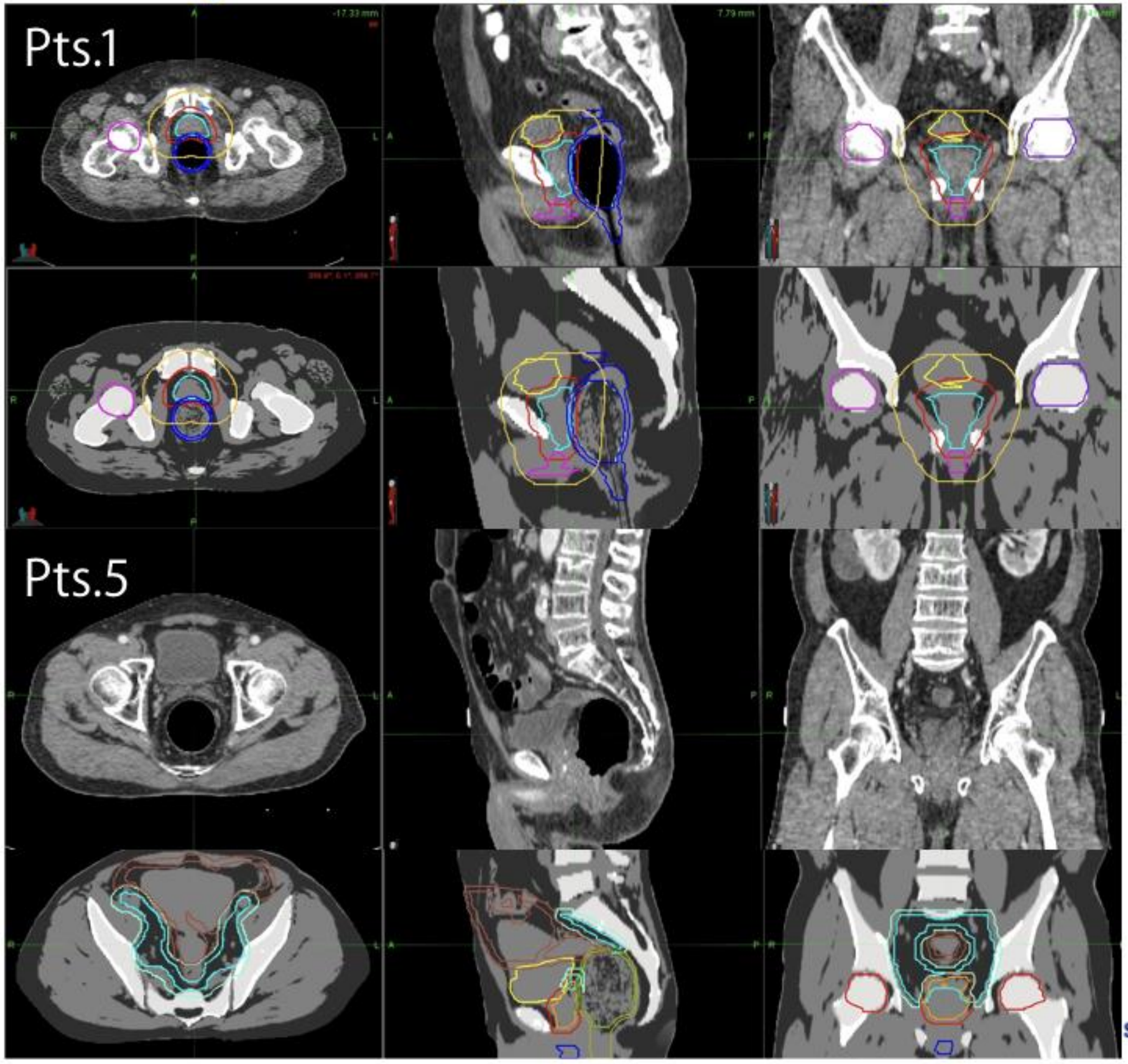

Comparison of Image Values

	planCT (HU)	synCT (HU)	Difference (HU)	*p*-values*
Target Volumes				
PTV1 (*n* = 16)	14.0 ± 24.9	23.4 ± 13.1	**9.5 ± 26.1**	0.07
PTV2 (*n* = 12)	33.4 ± 14.2	-6.8 ± 8.0	**-30.2 ± 20.3**	**< 0.01**
Normal Organs (*n* = 16)				
Bladder	18.6 ± 7.1	35.3 ± 6.1	**16.7 ± 10.5**	**< 0.01**
Rectum Wall	-143.3 ± 156.6	4.6 ± 10.3	**147.9 ± 154.4**	**< 0.01**
Femoral Head				
Right	279.5 ± 45.8	175.5 ± 6.1	**-104.0 ± 47.5**	**< 0.01**
Left	280.4 ± 50.5	177.7 ± 6.4	**-102.7 ± 51.7**	**< 0.01**
Penile Bulb	48.3 ± 14.7	40.3 ± 2.5	**-8.0 ± 14.0**	**0.02**
Fat and Muscle Volumes (*n* = 16)				
Fat	-69.4 ± 13.6	-77.3 ± 1.4	**-7.9 ± 13.0**	**0.02**
Muscle	34.1 ± 12.4	39.8 ± 0.4	**5.7 ± 12.3**	**0.05**

*Wilcoxon paired signed rank test was used.

Comparison of Dosimetric Parameters

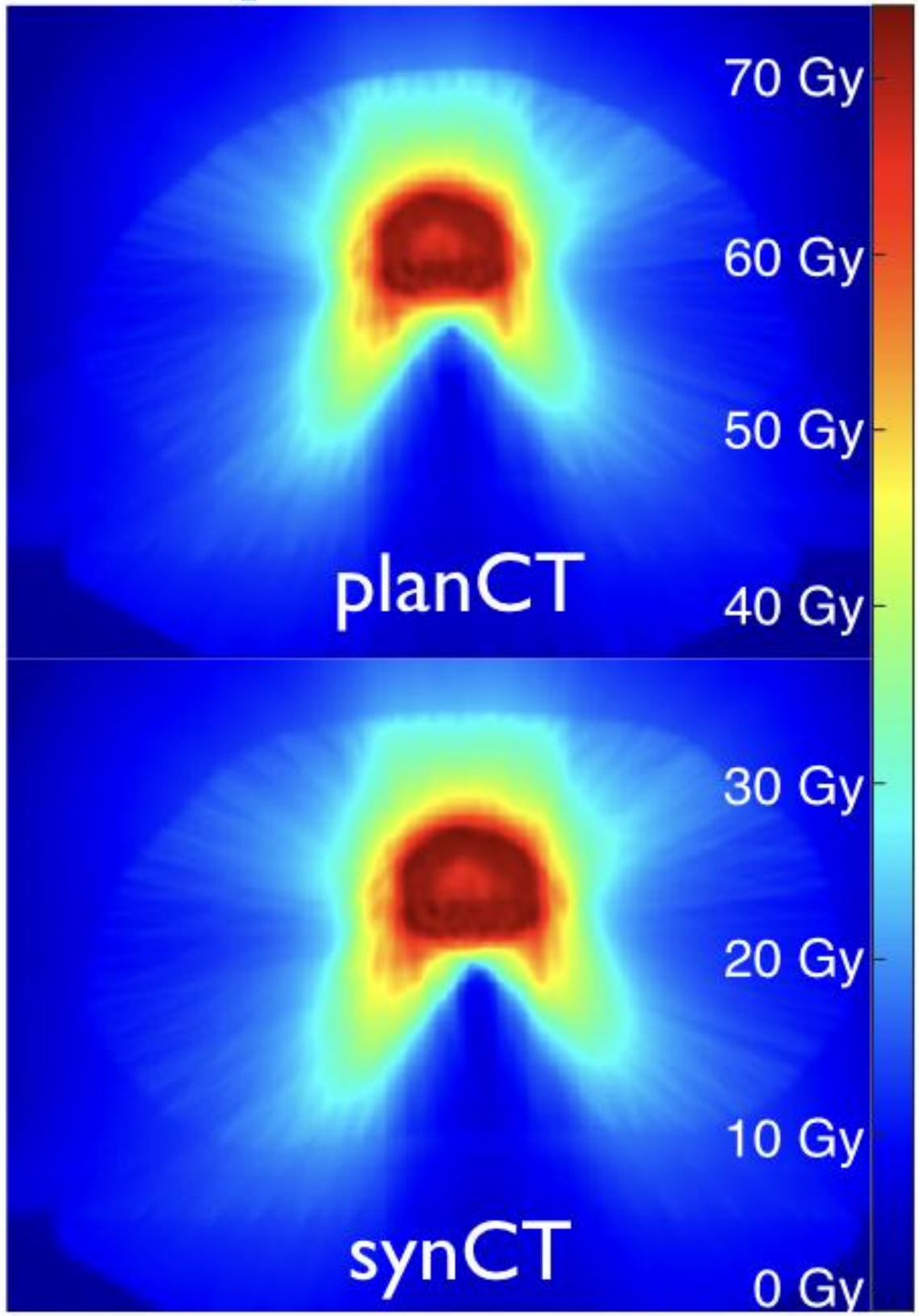

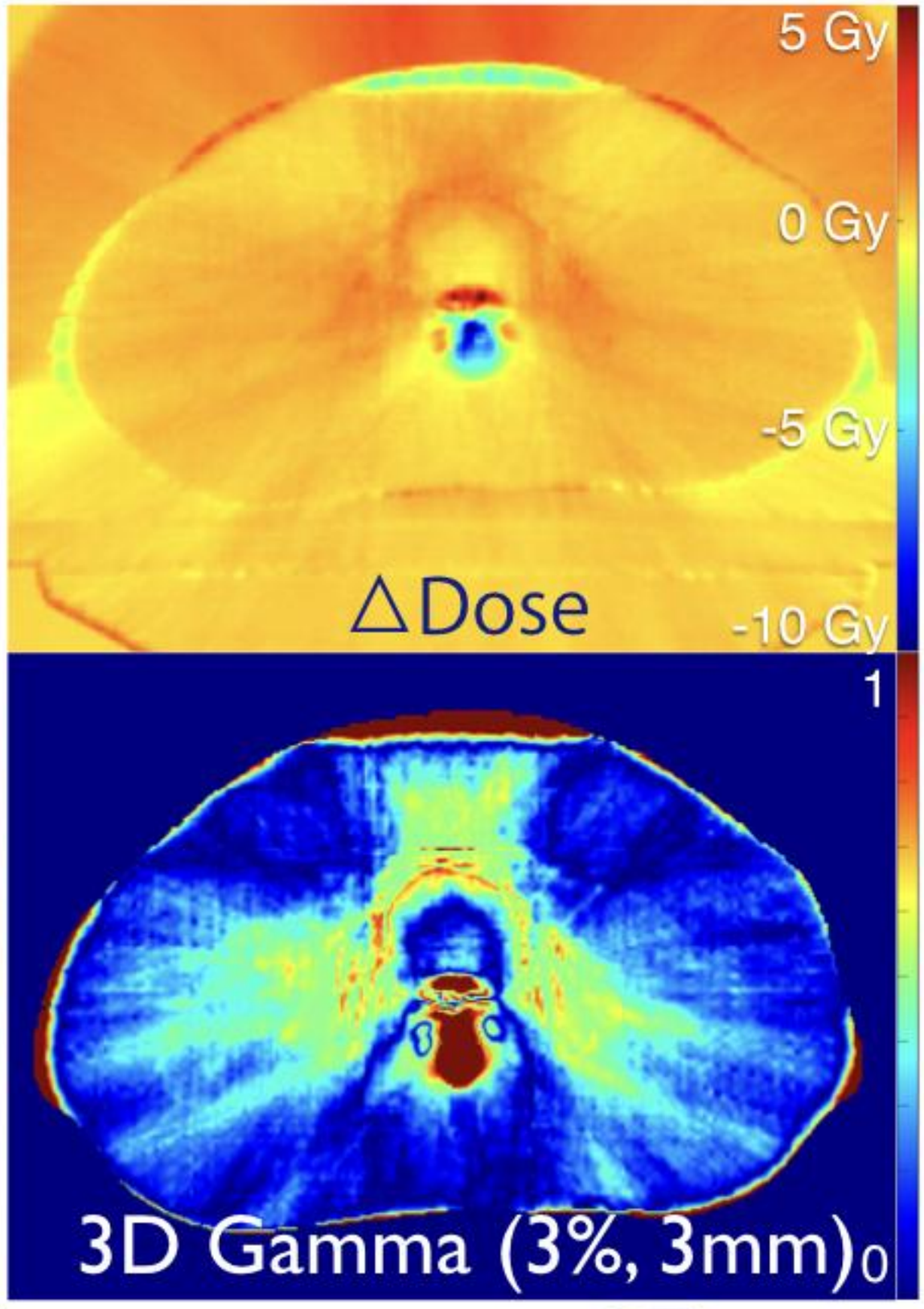

Comparison of Dosimetric Parameters

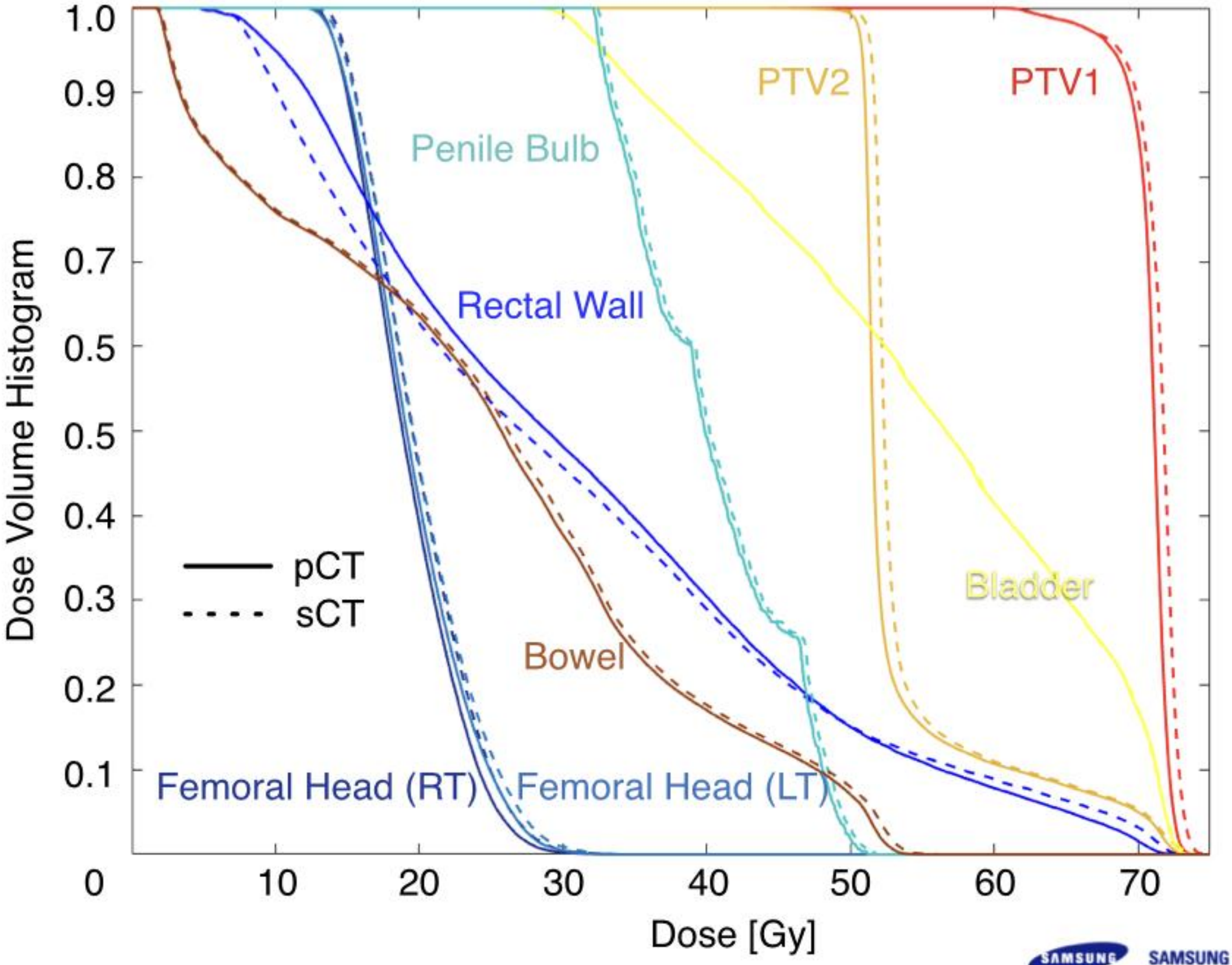

Comparison of Dosimetric Parameters

	planCT (Gy)	synCT (Gy)	Difference (Gy)	Normalized Difference (%)	*p*-values*
Target Volumes					
PTV1 (*n* = 16)					
Dmean	70.00 ± 0.61	70.46 ± 1.07	0.46 ± 0.77	(0.65% ± 1.11%)	**0.03**
D95%	67.86 ± 2.19	68.20 ± 2.17	0.33 ± 0.84	(0.48% ± 1.19%)	0.16
D5%	71.47 ± 0.79	72.20 ± 1.16	0.73 ± 0.74	(1.04% ± 1.05%)	**< 0.01**
PTV2 (*n* = 12)					
Dmean	50.92 ± 1.01	51.24 ± 1.21	0.32 ± 0.50	(0.34% ± 0.65%)	0.06
D95%	47.17 ± 2.44	47.33 ± 2.45	0.12 ± 0.48	(0.17% ± 0.68%)	0.34
D5%	57.28 ± 5.14	57.75 ± 5.24	0.35 ± 0.47	(0.50% ± 0.67%)	**< 0.01**
Fat and Muscle Volumes (*n* = 16)					
Fat					
Dmean	11.16 ± 4.00	11.28 ± 4.04	0.12 ± 0.08	(0.17% ± 0.11%)	**< 0.01**
Dmax	46.65 ± 9.14	47.02 ± 9.26	0.37 ± 0.51	(0.53% ± 0.73%)	**0.01**
Muscle					
Dmean	12.66 ± 4.15	12.81 ± 4.19	0.16 ± 0.09	(0.22% ± 0.13%)	**< 0.01**
Dmax	54.16 ± 7.51	54.78 ± 7.79	0.62 ± 0.69	(0.88% ± 0.99%)	**< 0.01**

Comparison of Dosimetric Parameters

	planCT (Gy)	synCT (Gy)	Difference (Gy)	Normalized Difference (%)	*p*-values*
Bladder					
Dmean	40.19 ± 7.19	40.28 ± 7.39	0.09 ± 0.52	(0.12% ± 0.75%)	0.98
Dmax	70.45 ± 1.00	70.55 ± 1.34	0.10 ± 0.80	(0.14% ± 1.14%)	0.97
Rectum Wall					
Dmean	30.72 ± 3.06	30.44 ± 2.89	-0.28 ± 0.44	(-0.41% ± 0.63%)	**0.03**
Dmax	70.02 ± 1.10	71.13 ± 1.65	1.11 ± 0.86	(1.59% ± 1.23%)	**< 0.01**
Right Femoral Head					
Dmean	21.35 ± 4.55	21.68 ± 4.64	0.33 ± 0.24	(0.48% ± 0.34%)	**< 0.01**
Dmax	34.92 ± 7.72	35.57 ± 7.98	0.65 ± 0.43	(0.93% ± 0.61%)	**< 0.01**
Left Femoral Head					
Dmean	20.93 ± 4.10	21.26 ± 4.19	0.33 ± 0.23	(0.47% ± 0.33%)	**< 0.01**
Dmax	34.53 ± 7.18	35.21 ± 7.48	0.67 ± 0.47	(0.96% ± 0.67%)	**< 0.01**
Penile Bulb					
Dmean	39.05 ± 14.86	39.46 ± 14.98	0.41 ± 0.41	(0.59% ± 0.59%)	**< 0.01**
Dmax	52.42 ± 14.84	52.97 ± 15.15	0.55 ± 0.69	(0.79% ± 0.98%)	**< 0.01**

Comparison of Dosimetric Parameters

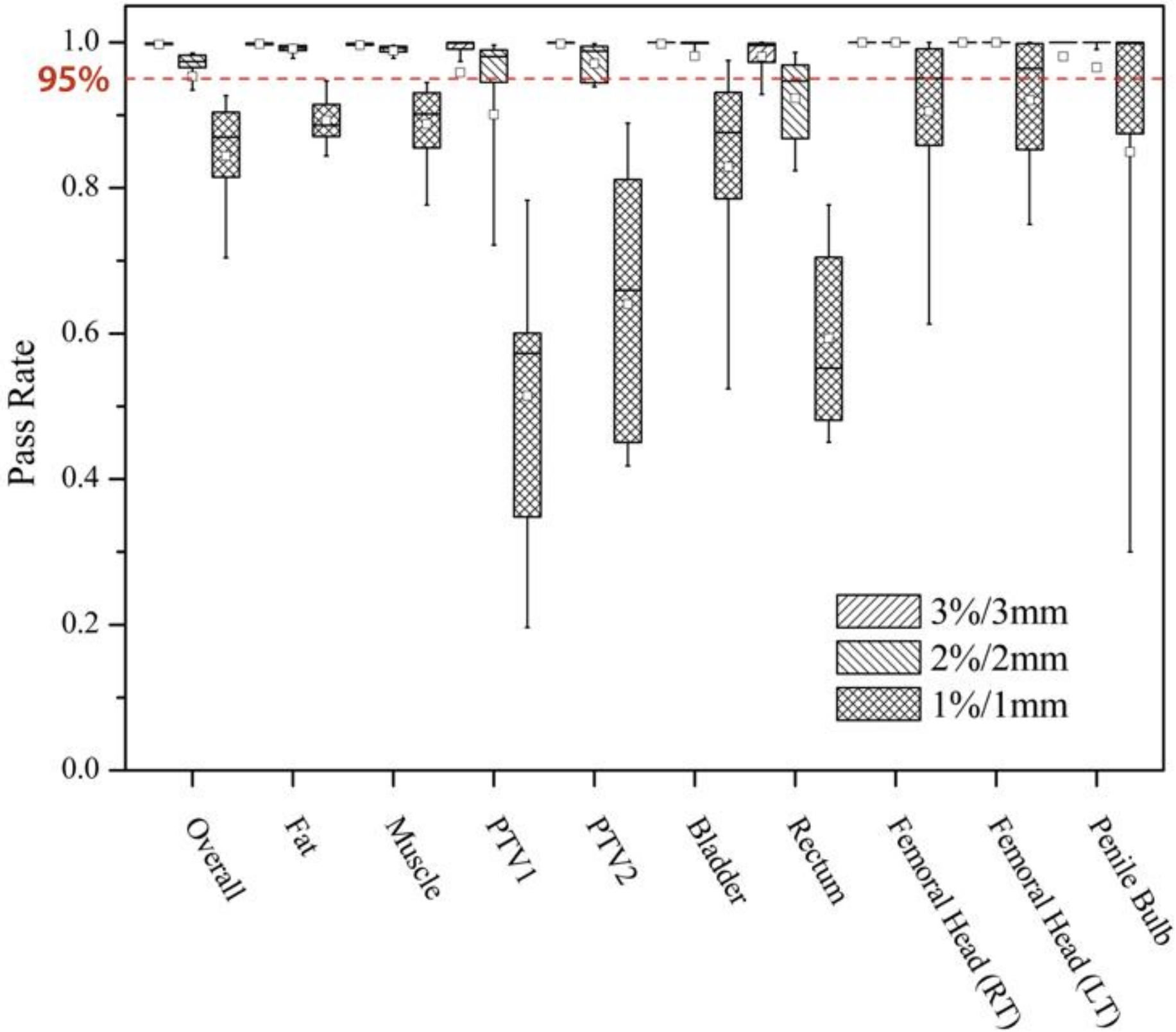

Comparison of Dosimetric Parameters

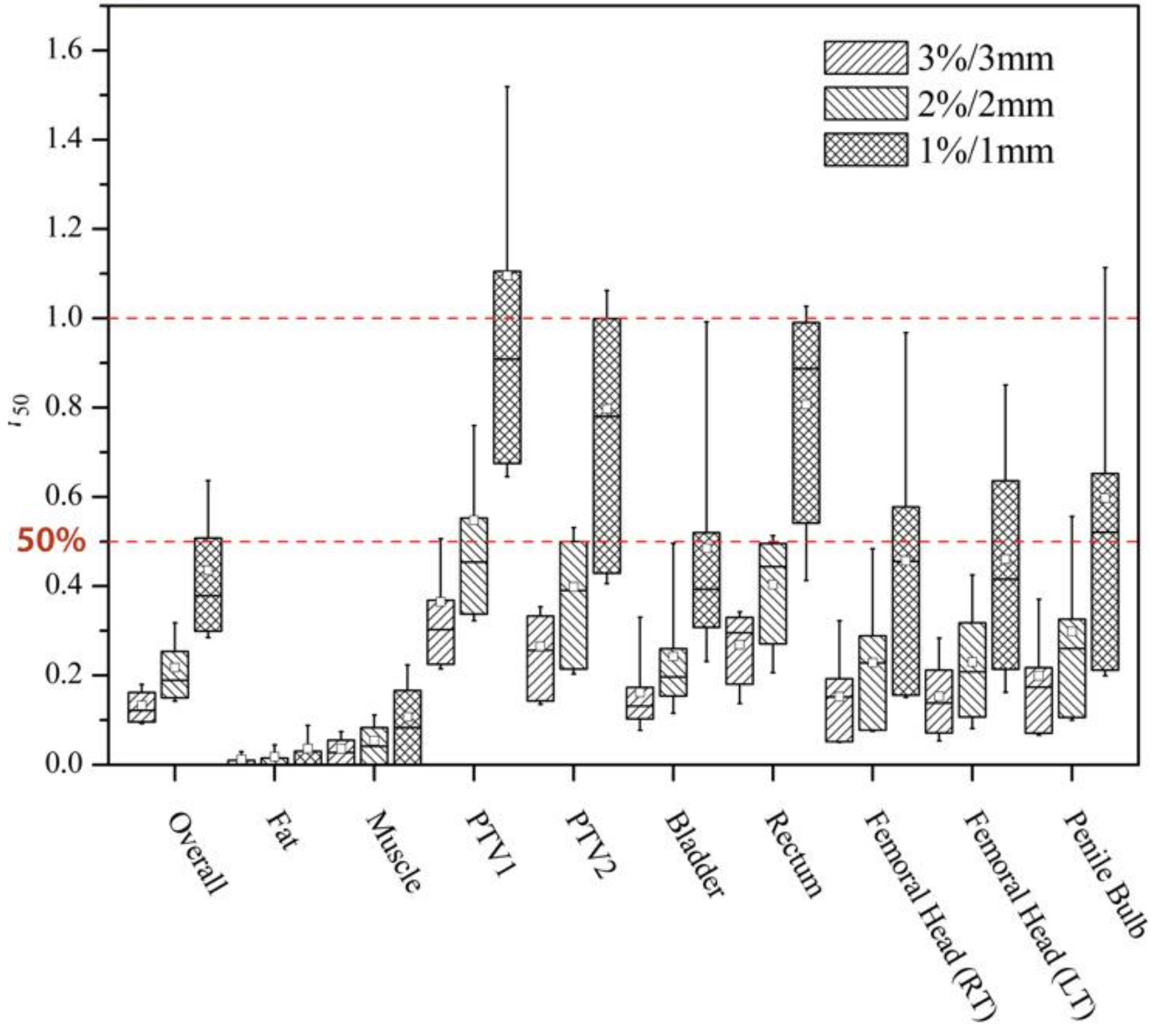

Consideration in MR Simulator

- Fraass BA, et al (1987): **Integration of magnetic resonance imaging into radiation therapy treatment planning: I. Technical considerations**
  - mechanically-obtained external contour and simulator film data,
  - The study has shown that to use MRI data for RTTP,
  - (a) **use careful patient positioning and marking**,
  - (b) transfer information from CT to MRI and vice versa,
  - (c) determine the **geometrical consistency** between the CT and MR data sets,
  - (d) investigate the **unwarping of distorted MR images**, and
  - (e) have the ability to **use non-axial images** for determination of beam treatment technique, dose calculations, and plan evaluation.

Geometrical Distortion

- Lack of Geometrical Validation
- Recently, B1 Calibration in Scan + Correction Map < sub-millimeters

T. Mizowaki, 1996

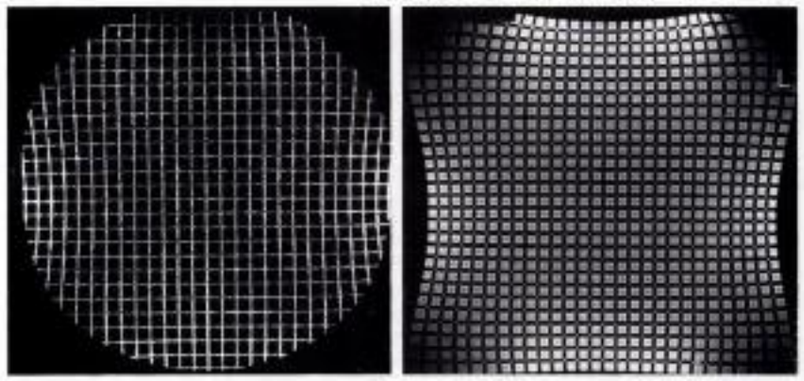

Figure 4. MR images of the two types of phantom. (a) T1-weighted axial images of the cylindrical phantom (FOV, 260 mm). (b) T1-weighted axial images of the cube-shaped phantom (FOV, 320 mm). Geometric distortion was generally observed in the peripheral area of the images. L = left.

Kim, H.Y., 2014

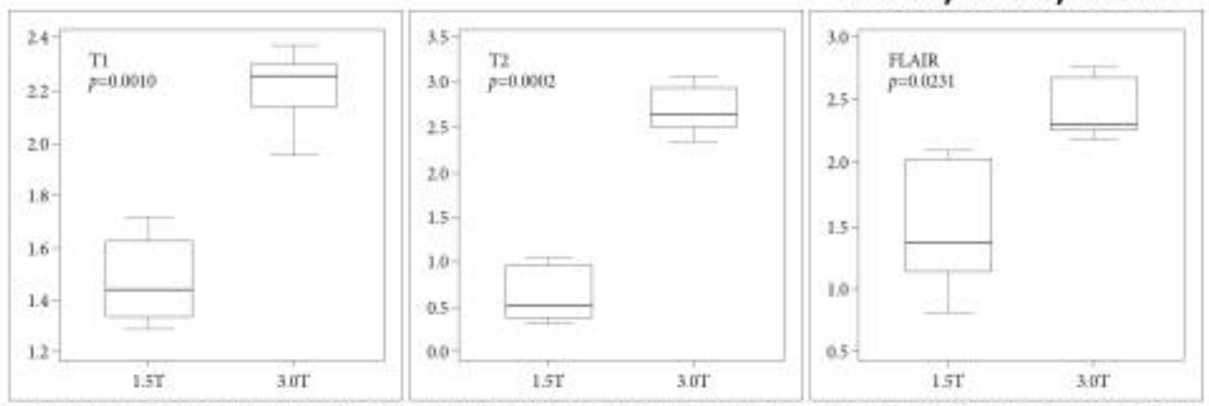

Fig. 4. The errors in the central area are shown in each MRI sequence. The difference between the 1.5T and 3.0T MRIs is statistically significant in all MRI sequences. All p-values are corrected by Bonferroni's method.

Torfeh, T., 2016

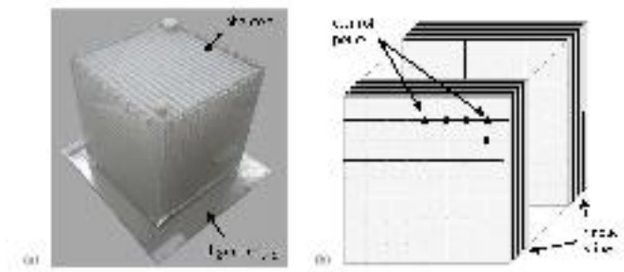

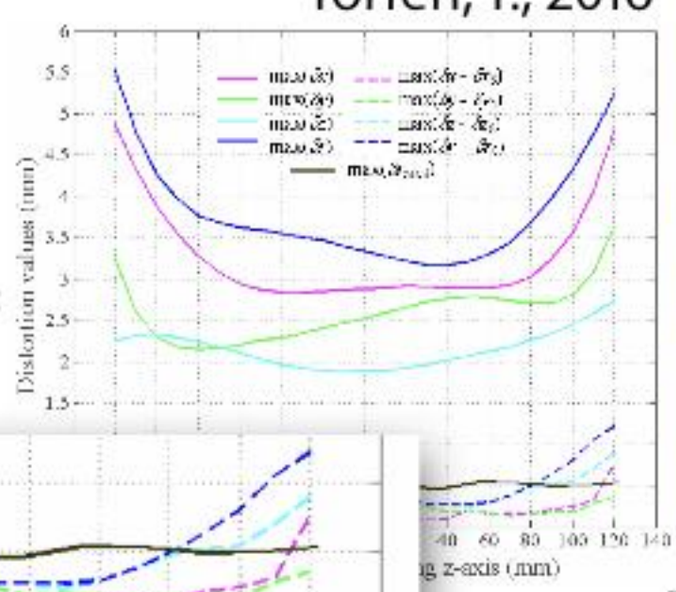

Torfeh, T., 2016

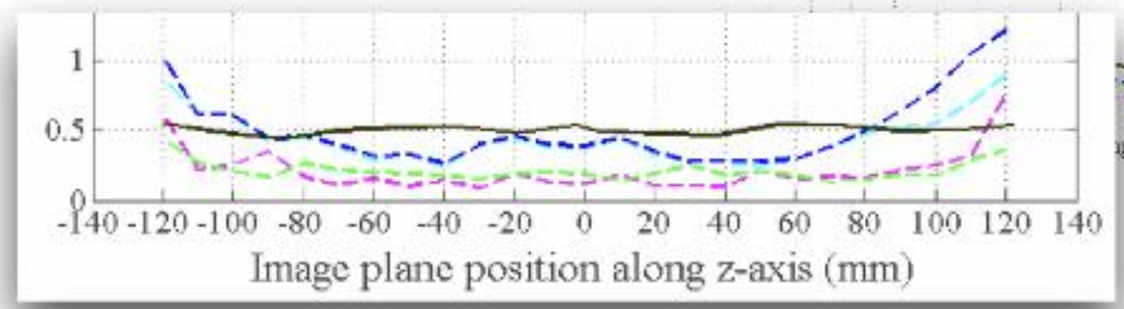

Baldwin, L.N. 2007

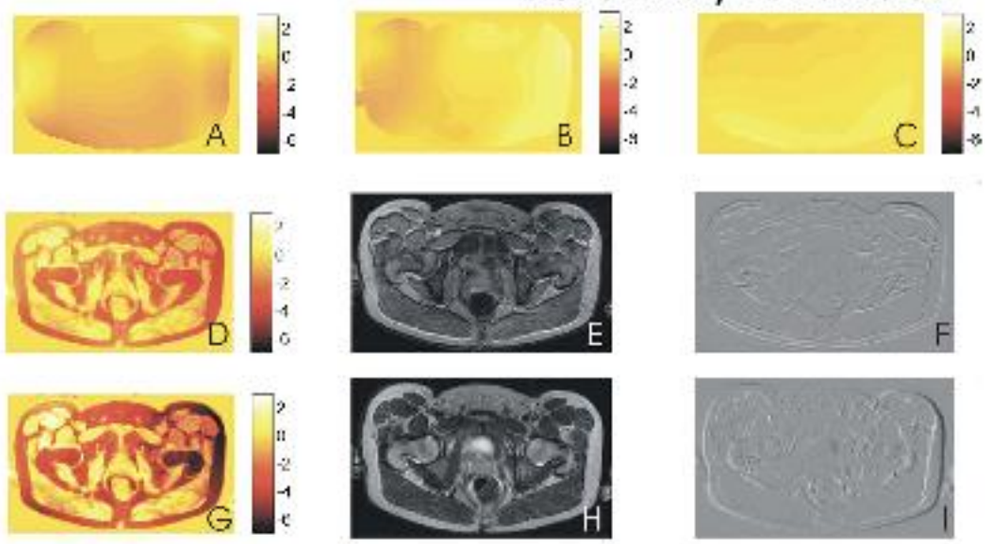

Fig. 7. Distortion correction for GE images [(d) and (e)] and SE images [(g)–(i)] of a male volunteer. (a) x-gradient nonlinearity distortions (mm). (b) y-gradient nonlinearity distortions (mm). (c) z-gradient nonlinearity distortions (mm). (d) Sequence-dependent spatial distortions (mm) for the GE sequence. (e) Original GE image. (f) Difference map (corrected—original). (g) Sequence-dependent distortions (mm) for the SE sequence. (h) Original SE image. (i) Difference map (corrected—original).

Quality Assurance using Dedicated Phantom

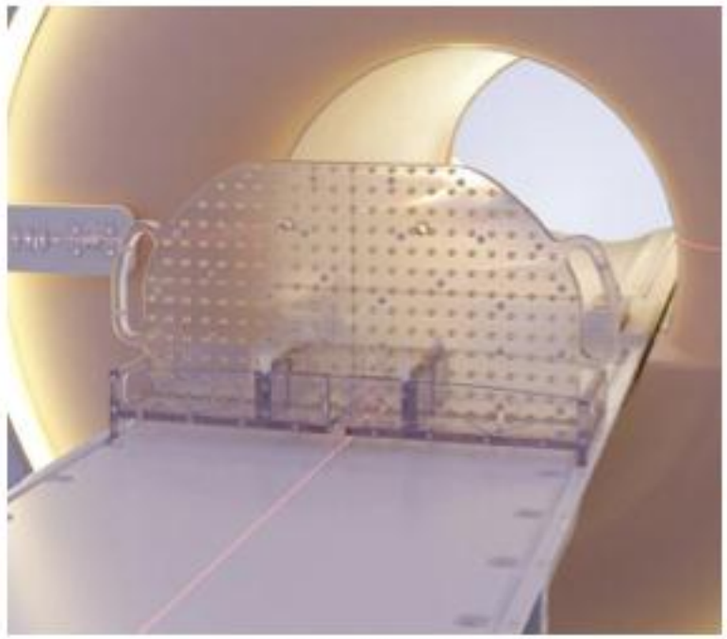

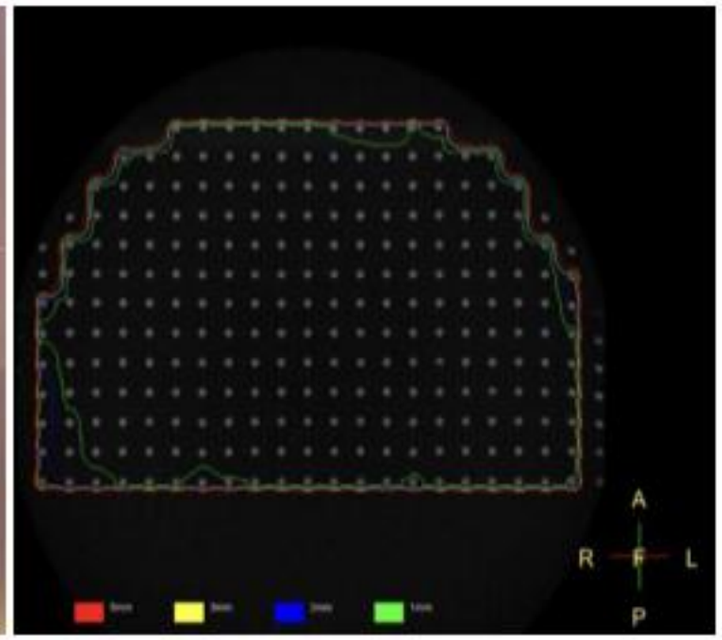

Geometric QA phantom and *rack*

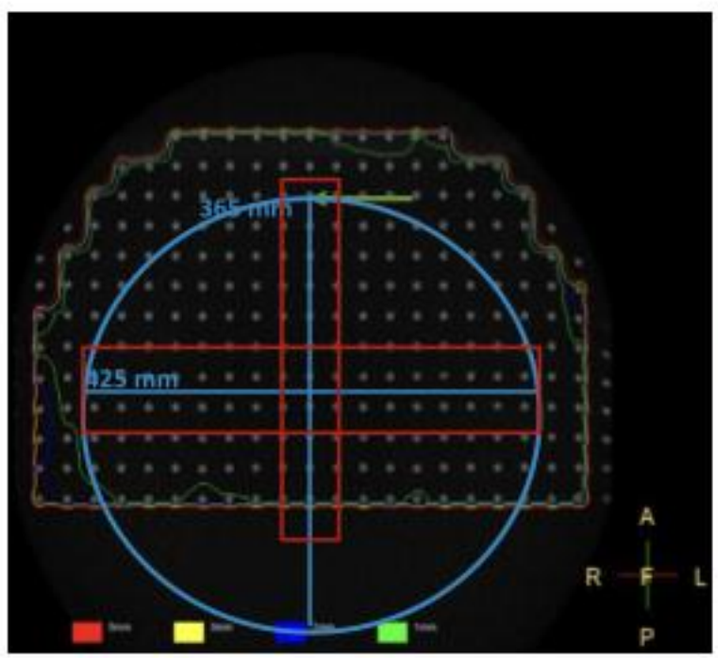

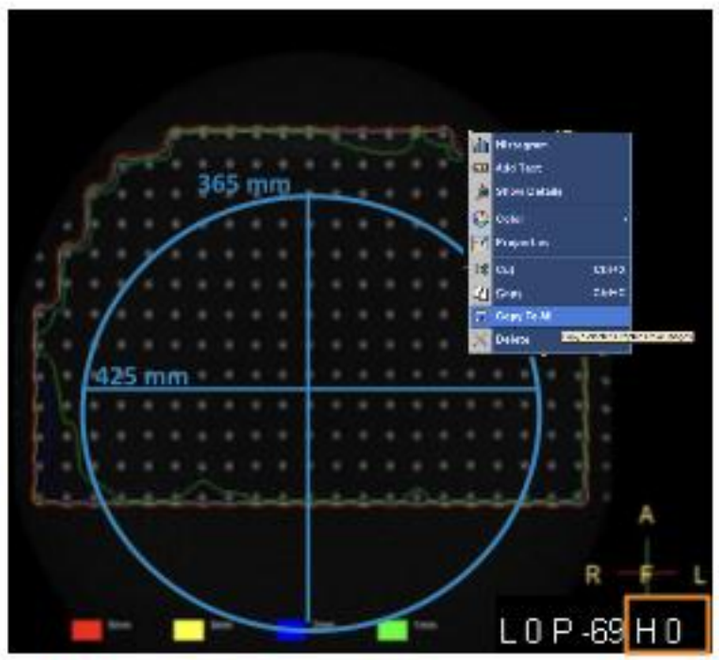

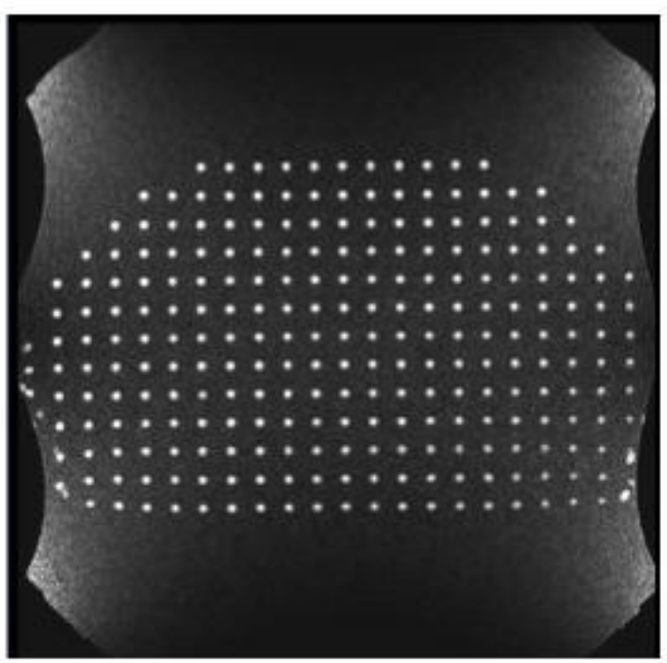

Quality Assurance using Dedicated Phantom

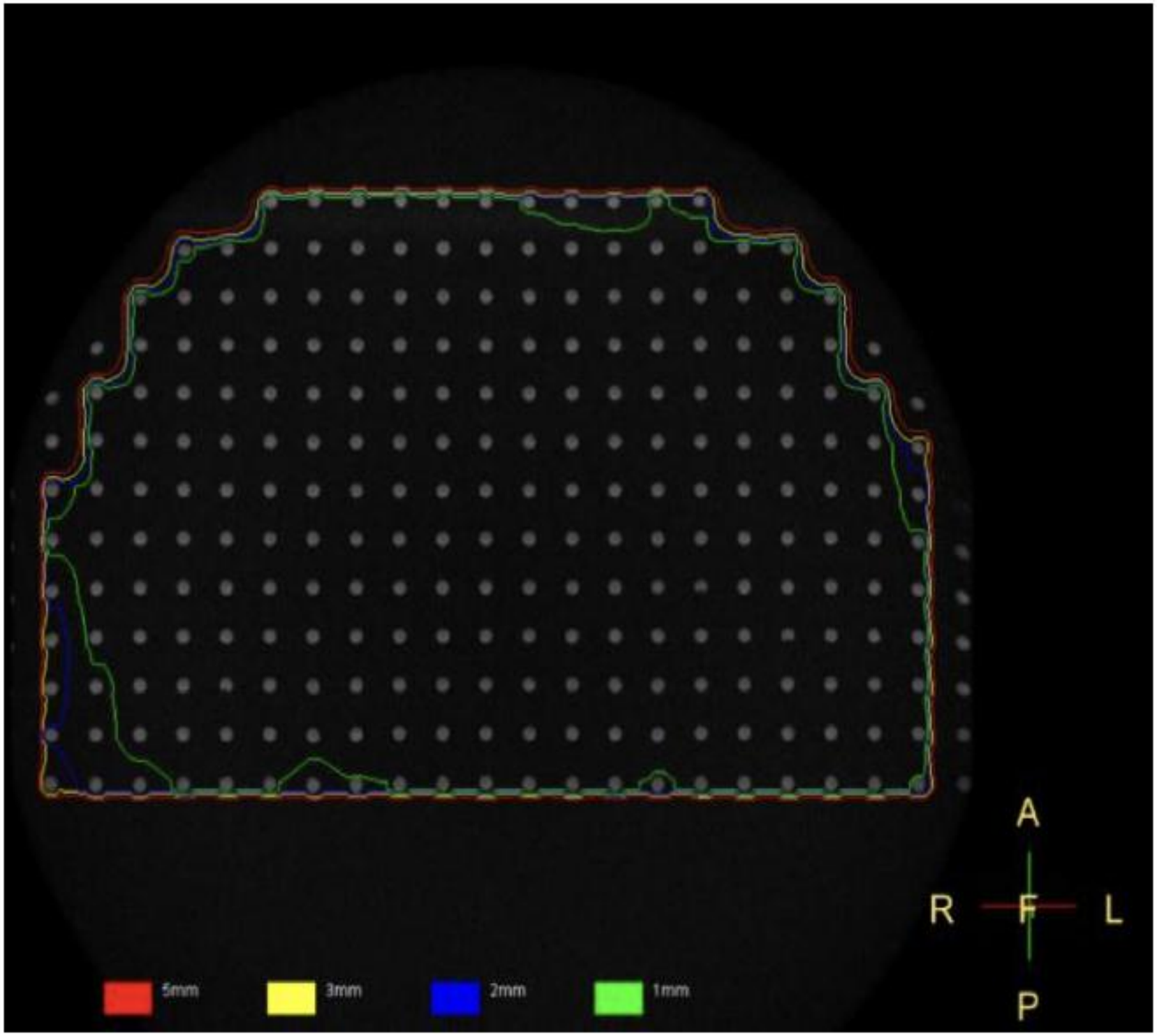

1 mm

2 mm

3 mm

5 mm

Quality Assurance using Dedicated Phantom

[redacted]

Maximum total distortions [mm]:

	All markers	DSV 500.0 mm	DSV 425.0 mm	DSV 365.0 mm	DSV 200.0 mm
dr	6.44	2.42	2.01	2.01	1.15
dr_discard	2.62	1.75	1.34	1.34	0.82

Maximum x, y, z distortions [mm]:

	All markers	DSV 500.0 mm	DSV 425.0 mm	DSV 365.0 mm	DSV 200.0 mm
dx	2.96	1.40	1.11	0.89	0.34
dy	5.61	1.99	1.99	1.99	1.13
dz	1.49	1.08	0.27	0.27	0.20
dx_discard	1.18	0.79	0.60	0.47	0.27
dy_discard	2.58	1.42	1.28	1.33	0.77
dz_discard	0.71	0.46	0.20	0.18	0.17

Number of markers found:

	All markers	DSV 500.0 mm	DSV 425.0 mm	DSV 365.0 mm	DSV 200.0 mm
n/N	250/251	214/214	162/162	119/119	35/35

SAMSUNG MEDICAL CENTER

Dose Difference due to ΔHU

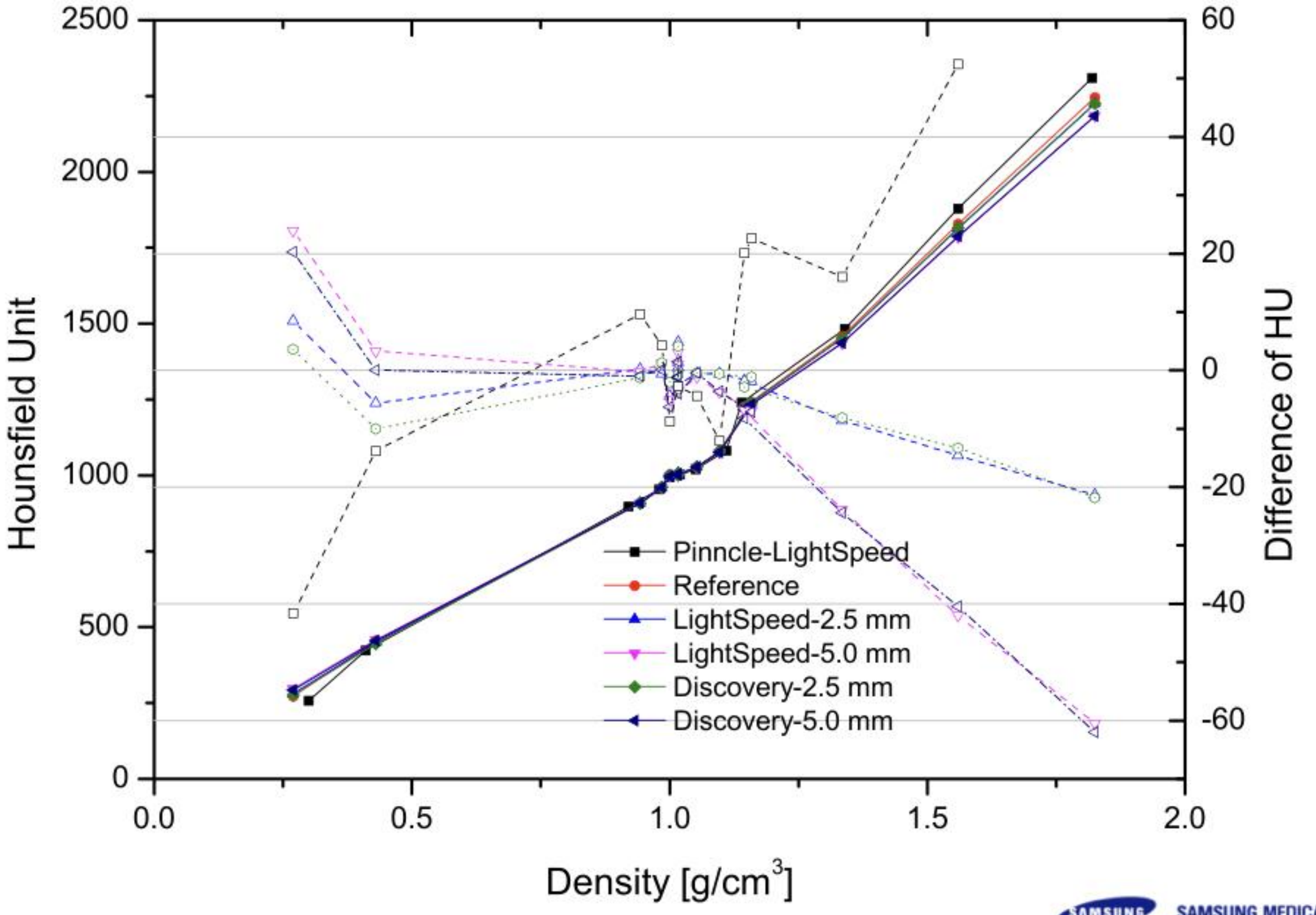

Dose Difference due to ΔHU

- 4MV, Brain and Lung Cases
- ΔHU 50 @ 0.3 g/cm3, ΔHU 90 @ 1.8 g/cm3

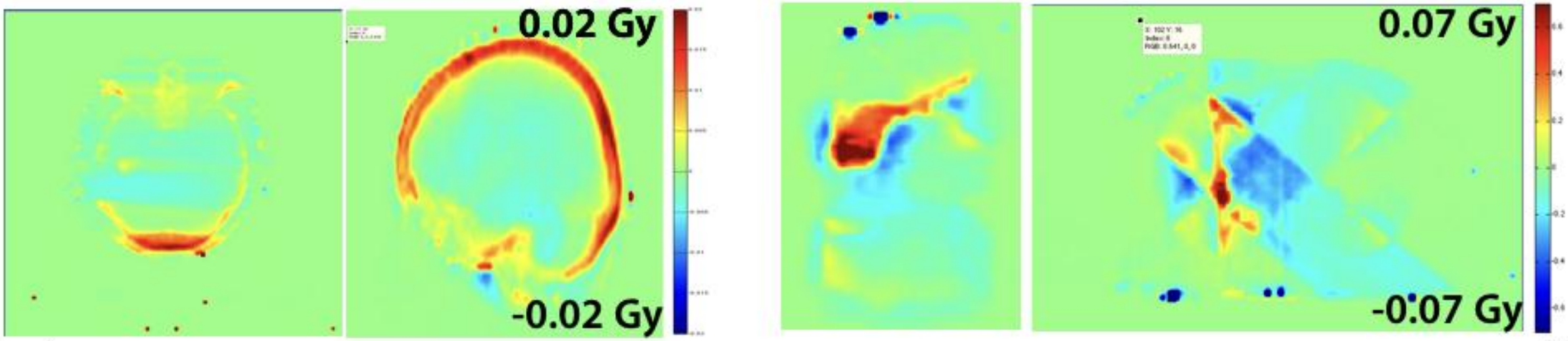

Brain [%]

	BRAIN	GTV	CTV	RT EYEBALL	LT EYEBALL	SPINAL CORD	BRAIN STEM	RT LENS	LT LENS	RT COCHLE	LT COCHLE	RT PAROTID	LT PAROTID	Body
Avg.	-0.07	0	0.01	-0.01	-0.02	-0.01	-0.03	-0.01	-0.02	0.49	0.58	0.02	0.01	0.02
Min	-0.32	-0.29	-1.23	-0.13	-0.14	-0.15	-0.3	-0.04	-0.03	0	0	-0.07	-0.13	-6.51
Max	0.49	0.62	4.32	0.23	0.11	0.05	0.43	0.03	0	0.71	0.78	0.2	0.57	53.73
Abs. Avg.	0.1	0.12	0.11	0.05	0.04	0.01	0.15	0.02	0.02	0.49	0.58	0.03	0.02	0.08

Lung [%]

	GTV	CTV	RT LUNG	LT LUNG	TRACHEA	ESOPHAGUS	SPINAL CORD	BOTH LUNG	Body
Avg.	-0.39	-0.35	0.03	-0.03	-0.13	-0.12	-0.09	0.01	-0.02
Min	-0.51	-0.6	-0.81	-0.43	-0.48	-0.52	-0.38	-0.81	-31.31
Max	0	0.49	1.31	0.46	0.31	0.03	0.03	1.31	9.61
Abs.Avg.	0.39	0.36	0.16	0.05	0.14	0.14	0.1	0.11	0.04

Image Guidance using synCT from MRCAT

- 25 prostate patients (intact gland or post-operative prostate bed)
- VMAT, 800 cGy × 5 fractions or 180 cGy × 40 fractions) or as a boost after permanent brachytherapy implant (500 cGy × 5 fractions)

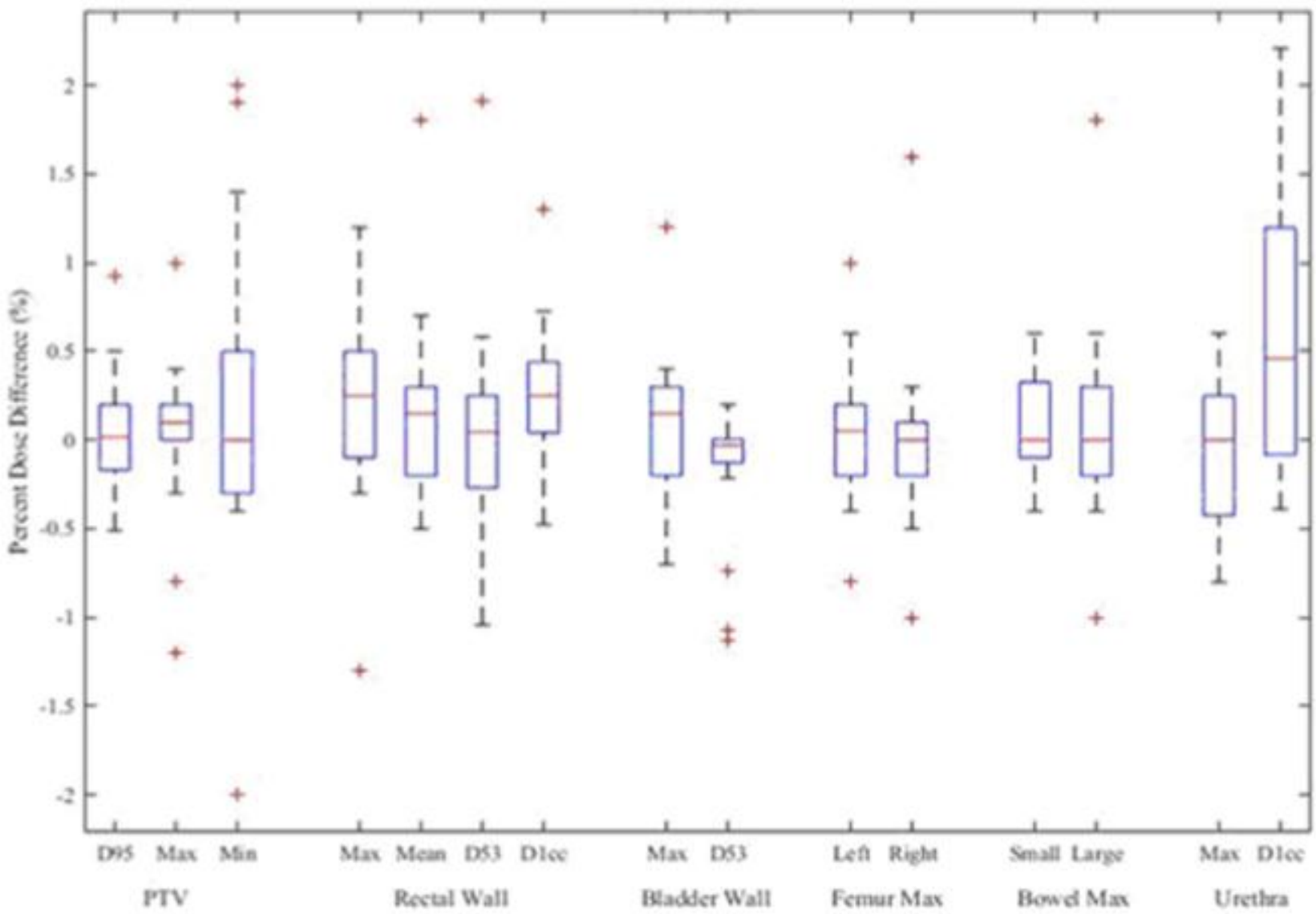

Tyagi N, et al. Phys Med Biol. 2017. 62(8).

SAMSUNG MEDICAL CENTER

Image Guidance using synCT from MRCAT

MRCAT DRR

CT DRR

Bony match

MRCAT DRR

KV radiograph

Fiducial match

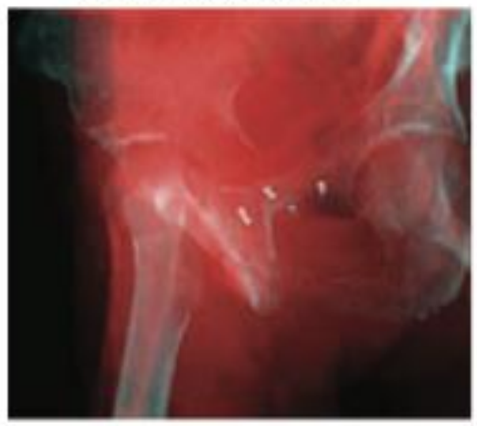

CT DRR

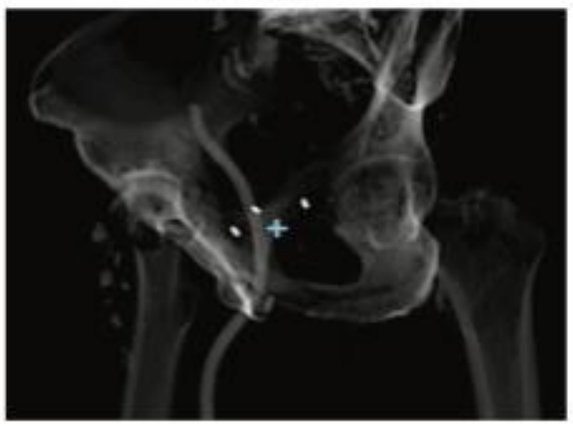

KV radiograph

Fiducial match

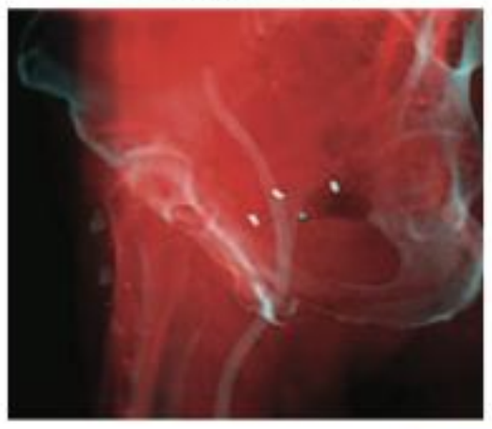

Tyagi N, et al. Phys Med Biol. 2017. 62(8).

SAMSUNG MEDICAL CENTER

Image Guidance using synCT from MRCAT

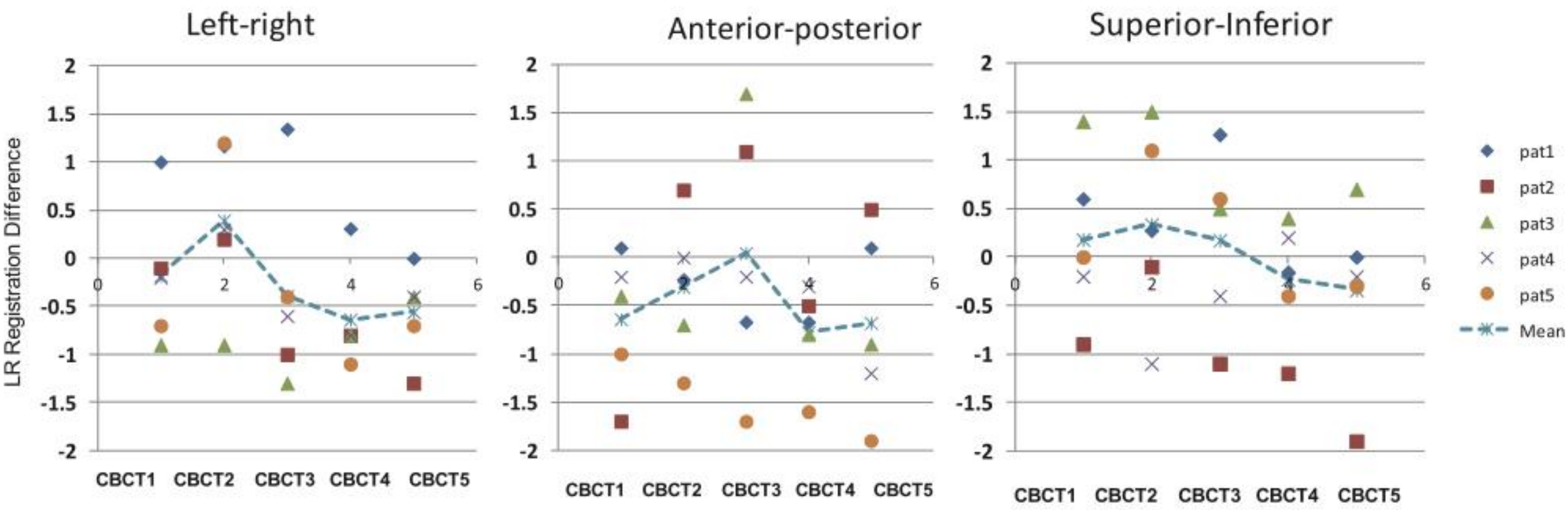

Figure 9. Difference between planning CT to CBCT (CT-CBCT) and MRCAT syn-CT to CBCT (MRCAT-CBCT) registrations for four patents undergoing hypofractionated image-guided prostate radiotherapy. The difference is calculated along the LR, AP and SI direction.

Tyagi N, et al. Phys Med Biol. 2017. 62(8).

Image Guidance using synCT from MRCAT

- We could not validate the feasibility of MRCAT based IGRT.
- We expected the more effective in TomoTherapy.

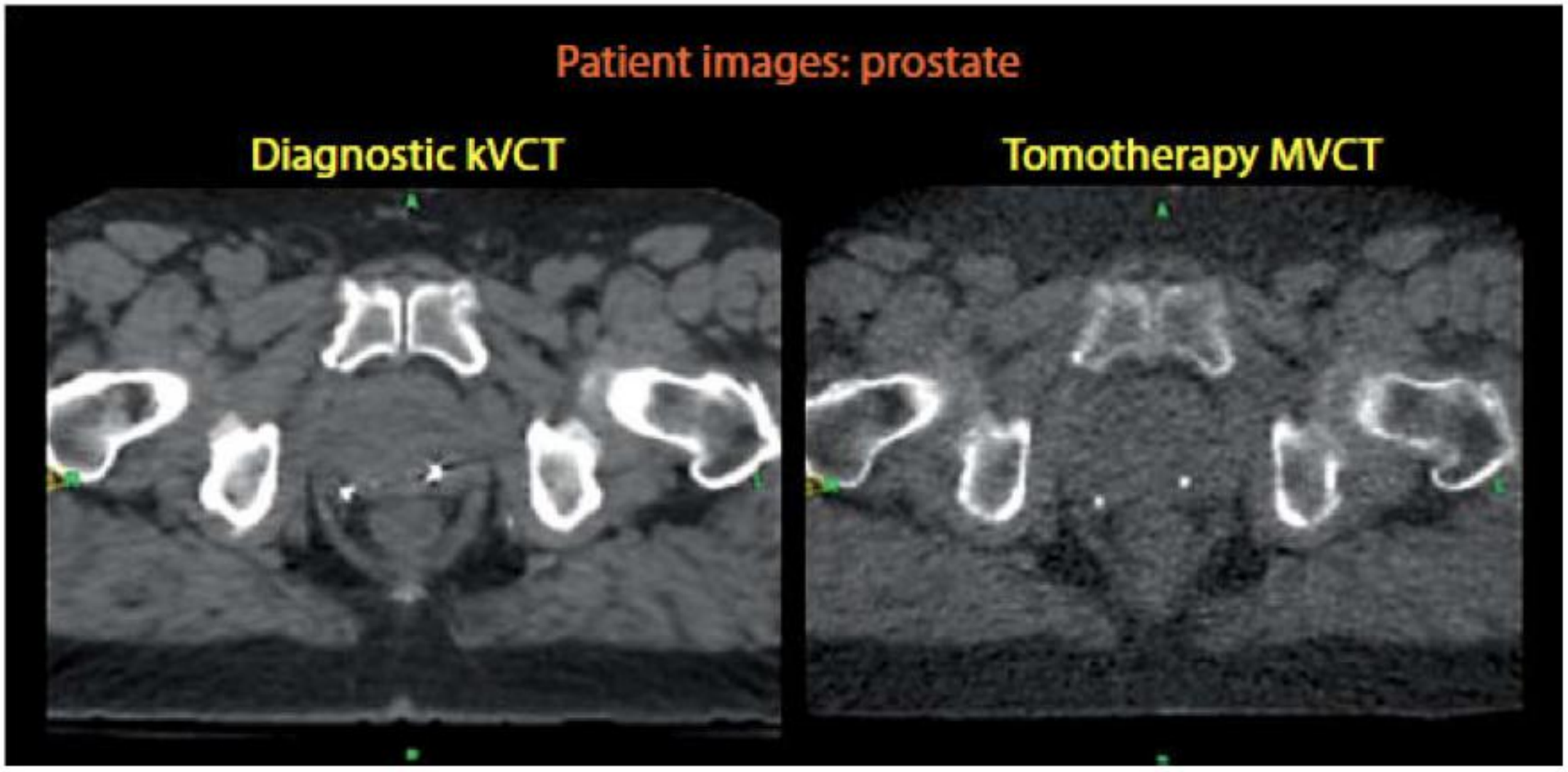

P. Kupelian and K. Langen, "Helical Tomotherapy: Image-Guided and Adaptive Radiotherapy," 2011).

Summaries

- Clinical Impact of MRCAT
  - synCT could be generated automatically without additional workload.
  - Imaging dose could be minimized in CT simulation.
  - Difference of dose exists with statistical significance, however, the difference is acceptable clinically (less than 1%).
- MR-only RT could be feasible clinically with good agreement of dose.
- MR-only RT planning should be designed carefully.
  - Body distortion due to immobilization or use of MR coil
  - Internal material inside body: air or gas
  - Image distortion due to implemented metal